Publications from Thesis

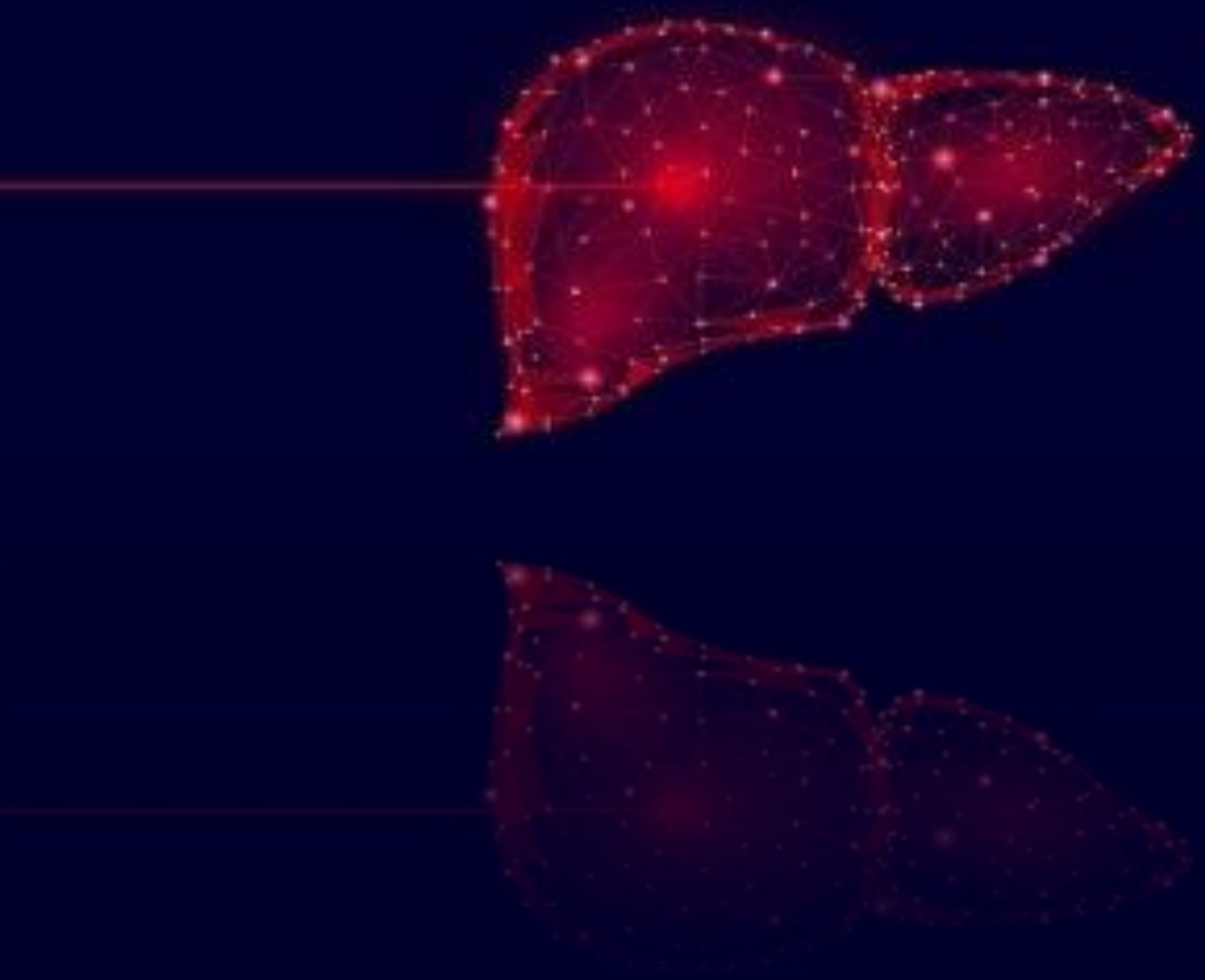

Toxicology and Applied Pharmacology 360 (2018) 99–108

Contents lists available at ScienceDirect

Toxicology and Applied Pharmacology

journal homepage: www.elsevier.com/locate/taap

Carbon monoxide releasing molecule A-1 attenuates acetaminophen-mediated hepatotoxicity and improves survival of mice by induction of Nrf2 and related genes

Kapil K. Upadhyay[a], Ravirajsinh N. Jadeja[b], Jaymesh M. Thadani[a], Apeksha Joshi[a], Aliasgar Vohra[a], Vishal Mevada[c], Rajesh Patel[d], Sandeep Khurana[e], Ranjitsinh V. Devkar[a,*]

[a] Phytotherapeutics and Metabolic Endocrinology Division, Department of Zoology, Faculty of Science, The Maharaja Sayajirao University of Baroda, Vadodara, Gujarat 390002, India
[b] Department of Biochemistry and Molecular Biology, Augusta University, Augusta, GA, 30912,USA
[c] Hemchandracharya North Gujarat University, Patan, Gujarat 384265, India
[d] Bioinformatics and Supercomputer lab, Department of Biosciences, Veer Narmad South Gujarat University, Surat, Gujarat 395007, India
[e] Division of Gastroenterology, Hepatology and Nutrition and Weight Management, Geisinger Medical Center, Danville, PA 17822, USA

ARTICLE INFO

Keywords:
CORM A-1
Acetaminophen
Liver
Nuclear Factor Erythroid 2-Related Factor 2
Kelch-Like ECH-Associated Protein 1

ABSTRACT

Acute liver injury is frequently associated with oxidative stress. Here, we investigated the therapeutic potential of carbon monoxide releasing molecule A-1 (CORM A-1) in oxidative stress-mediated liver injury. Overnight-fasted mice were injected with acetaminophen (APAP; 300 mg/kg; intraperitoneally) and were sacrificed at 4 and 12 h. They showed elevated levels of serum transaminases, depleted hepatic glutathione (GSH) and hepatocyte necrosis. Mice injected with CORM A-1 (20 mg/kg) 1 h after APAP administration, had reduced serum transaminases, preserved hepatic GSH and reduced hepatocyte necrosis. Mice that received a lethal dose of APAP (600 mg/kg), died by 10 h; but those co-treated with CORM A-1 showed a 50% survival. Compared to APAP-treated mice, livers from those co-treated with CORM A-1, had upregulation of Nrf2 and ARE genes (HO-1, GCLM and NQO-1). APAP-treated mice had elevated hepatic mRNA levels of inflammatory genes (Nf-κB, TNF-α, IL1-β and IL-6), an effect blunted in those co-treated with CORM A-1. In *tert*-butyl hydroperoxide (t-BHP)-treated HepG2 cells, CORM A-1 augmented cell viability, reduced oxidative stress, activated the nuclear factor erythroid 2–related factor 2 (Nrf2) and anti-oxidant response element (ARE) genes. The molecular docking profile of CO in the kelch domain of Keap1 protein suggested that CO released from CORM A-1 mediated Nrf2 activation. Collectively, these data indicate that CORM A-1 reduces oxidative stress by upregulating Nrf2 and related genes, and restoring hepatic GSH, to reduce hepatocyte necrosis and thus minimize liver injury that contributes to an overall improved survival rate.

1. Introduction

Liver detoxifies endogenous metabolites and xenobiotics generated after medication ingestion and thus remains at risk for injury due to generation of free radicals or reactive oxygen species (ROS) (Yan et al., 2009). Liver has a robust antioxidant defense system that plays key role in modulating drug-induced liver injury (DILI) (Zhu et al., 2012). Therefore, hepatoprotective agents—that enhance cellular antioxidant defense system, scavenge free radicals and reduce the risk of ROS induced damage—have potential in treating DILI (Jadeja et al., 2016a). Acetaminophen (*N*-acetyl-p-aminophenol, APAP) is a widely used antipyritic whose overdose is the most common cause of DILI (Nourjah et al., 2006; Liu et al., 2012; Urrunaga et al., 2015). After APAP overdose, the sulfation and glucuronidation pathways are saturated leading to increased APAP metabolism by hepatic cytochrome P-450 (CYP450) (Urrunaga et al., 2015). This leads to generation of *N*-acetyl-p-benzoquinone imine (NAPQI), a highly toxic metabolite that depletes GSH stores, binds to cellular proteins and induces necrosis, which initiates sterile inflammation (Knight et al., 2002; Saito et al., 2010; Jaeschke et al., 2012a). *N*-acetyl cysteine (NAC), a precursor of cellular GSH biosynthesis, is the only FDA-approved antidote for APAP-induced hepatotoxicity (Heard and Green, 2012). However, NAC has a narrow rescue window; treatment response is best when NAC is administered within 8 h of APAP overdose (Kerr et al., 2005; Whyte et al., 2007).

* Corresponding author.
E-mail address: rv.devkar-zoo@msubaroda.ac.in (R.V. Devkar).

https://doi.org/10.1016/j.taap.2018.09.034
Received 14 June 2018; Received in revised form 21 September 2018; Accepted 23 September 2018
Available online 28 September 2018
0041-008X/ © 2018 Elsevier Inc. All rights reserved.

There are rare reports of NAC mediated side-effects (vomiting, nausea and shock) (Network, 2010).

Nuclear erythroid 2-related factor 2 (Nrf2), a transcriptional factor, is the major regulator of oxidative stress in hepatocytes. Nrf2 protects against APAP-induced oxidative stress and liver injury by increasing the expression of both metabolizing enzymes and ARE genes [viz. NAD(P)H:quinine oxidoreductase 1 (NQO1), glutamate-cysteine ligase – catalytic and modifier subunits (GCLC and GCLM) and heme oxygenase-1 (HO-1)] (Kay et al., 2011; Mani et al., 2013; Espinosa-Diez et al., 2015). Therefore, in models of liver injury, a variety of Nrf2 activators such as phytochemicals (Jadeja et al., 2016a), drugs (Zhang et al., 2017) or gases (Liu et al., 2012; Iwakiri and Kim, 2015) have been investigated for their therapeutic potential. In animal models, nitric oxide donor or hydrogen sulphide alleviates APAP-induced liver injury thus providing evidence that gasotransmitters may have a therapeutic potential (Liu et al., 2003; Morsy et al., 2010).

Physiological role of carbon monoxide (CO) as a regulator of cellular function is well- investigated (Ryter et al., 2006). CO is easily diffusible across cellular and biological membranes and therefore can mediate functional changes rapidly (Motterlini and Otterbein, 2010). Some known CO targets include soluble guanyl cyclase, heme containing potassium channels, transcriptional factors (BACH1 and NPAS-2), caveolae, nitric oxide synthase (NOS) and NADPH oxidase (Boczkowski et al., 2006). CO also interacts with cellular components lacking transitional metal (Otterbein et al., 2000; Zhang et al., 2004).

Carbon monoxide releasing molecules (CORMs) with a core of third transitional metal such as manganese or ruthenium are fast releasers of CO (Motterlini et al., 2002; Motterlini et al., 2003). Carbon monoxide releasing molecule A-1 (CORM A-1) has a boron core and releases CO slowly ($t_{1/2}$ = 21 min). It is water soluble and has been investigated for its therapeutic effect in diabetes (Nikolic et al., 2015), myocardial infarction (Varadi et al., 2007), posterior uveitis (Fagone et al., 2015) and neurogenesis (Almeida et al., 2016). In addition to preclinical studies, clinical trials have been initiated to examine safety and efficacy of CO in patients with idiopathic pulmonary fibrosis, pulmonary arterial hypertension, lung inflammation and acute respiratory distress syndrome (ClinicalTrials.gov., 2015d; ClinicalTrials.gov., 2015a; ClinicalTrials.gov., 2015b; ClinicalTrials.gov., 2015c). Unlike other gasotransmitters such as NO and H_2S, CO is more stable and its action is specific to transition metals.

We hypothesized that CO modulates oxidative stress in liver injury. To test this hypothesis, we conducted a proof-of-concept investigation to determine the effects of CORM A-1 in two established models of oxidative stress-mediated liver injury viz. t-BHP-induced injury in HepG2 cells and APAP-induced liver injury in mice model.

2. Materials and methods

2.1. Materials

CORM A-1, hematoxylin, eosin and APAP were purchased from Sigma Aldrich (St. Louis, MO, USA). Methanol, dimethyl sulphoxide (DMSO), 3-(4,5-dimethylthiazol-2-yl)-2,5-diphenyl tetrazolium bromide (MTT), tert-Butyl hydroperoxide (t-BHP) and DTNB or Elman's reagent were purchased from Sisco Research Laboratory Pvt. Ltd. (Mumbai, India). Dulbecco's Modified Eagle's Medium (DMEM), fetal bovine Serum (FBS), trypsin phosphate versene glucose (TPVG) and antibiotic-antimycotic solution were purchased from Hi-media Laboratories (Mumbai, India). ENZOPAK AST, ALT, ALP kits were purchased from Reckon Diagnostics (Vadodara, Gujarat). Molecular biology reagents except iScript cDNA synthesis kit (Bio-Rad, CA, USA) and all other reagents such as TRIzol, DreamTaq Green master mix and SYBR select master mix were procured from Invitrogen (CA, USA). RNA-later was purchased from Ambion Inc. (USA). Antibodies for Nrf2, HO-1 and β-actin proteins and secondary (anti-rabbit) antibody were purchased from Cell Signaling Technology, U.S.A. whereas, antibody for Lamin B was from Abcam U.K.

2.2. Maintenance of HepG2 cells and treatment schedules

Human Hepatoma (HepG2) cells were procured from National Centre for Cell Science (NCCS, Pune, India) and maintained in CO_2 incubator (Thermo scientific, forma series II 3110, USA) at 37 °C with 5% CO_2 in DMEM (10% FBS and 1% antibiotic antimycotic solution). Cells were sub-cultured using 1× TPVG every third day. To assess cytotoxicity, cells were treated with 5, 10, 25 and 50 μM t-BHP alone or with CORM A-1 (100 μM) for 2 h. Cells were also treated with CORM A-1 alone (10–100 μM).

2.3. Cytotoxicity and intracellular reactive oxygen species assay

HepG2 cells were seeded in 96-well plates (10^4 cells/well), allowed to grow overnight and were treated with t-BHP (5, 10, 25, 50 μM) in the absence or presence of CORM A-1 (100 μM) for 2 h. Later, cells were incubated with MTT (5 mg/ml) for 4 h and resultant crystals of formazan were dissolved in DMSO (150 μl/well). Absorbance measured at 540 nm using Synergy HTX Multimode Reader (Bio-Tek instruments, Inc., Winooski, VT), and cell viability calculated (% control).

HepG2 cells treated with t-BHP and CORM A-1 were also stained with 10 μM 2, 7-dichlorodihydrofluoroscein diacetate (CM-H2-DCFDA) at 37 °C for 30 min. Cells were photographed (EvosFloid cell imaging station; Life technologies, USA) and the intracellular fluorescence quantified using Image J software.

2.4. Experimental animals

Experimental protocol was approved by Institutional Animal Ethical Committee (IAEC) (Approval no. MSU-Z/IAEC-2/09–2018) and all experiments were conducted in CPCSEA-approved *(827/GO/Re/S/04/CPCSEA)* animal house facility at the Department of Zoology, The Maharaja Sayajirao University of Baroda, Vadodara, Gujarat, India. Swiss albino male mice (n = 42, 6–8 wks old, 25–30 g each) were procured (Flair lab, Surat, Gujarat, India) and maintained as per standard guidelines (23 ± 2 °C, LD 12:12, laboratory chow and water ad libitum). All experiments were performed after acclimatization for 1 week.

2.5. Acetaminophen-induced liver injury and CORM A-1 treatment

APAP dose (300 mg/kg), route of administration (*i.p.*) and time of sacrifice were used as described previously by James et al., 2003 (James et al., 2003). Overnight fasted mice were divided into seven groups (n = 6). Group 1: Untreated; Group 2: Saline treated; Group 3: APAP (4 h); Group 4: APAP + CORM A-1 (4 h); Group 5: APAP (12*h*); Group 6: APAP + CORM A-1 (12 h); Group 7: iCORM A-1 (12 h). APAP (300 mg/kg) was injected intraperitoneally and CORM A-1 (20 mg/kg) was administered one hour later (Fig. 1). Literature suggests varied doses of CORM A-1 (2 mg/kg every day/twice a day or a single dose of 60 mg/kg) in mice depending on the experimentally induced disease scenario (Lee et al., 2006; Urquhart et al., 2007; Hosick et al., 2014; Nikolic et al., 2014; Mangano et al., 2018). In a pilot experiment, we had used 2 mg/kg dose of CORM A-1 that had minimal effect on APAP-induced liver injury in mice (data not shown here). Since CORM A-1 has a very short half-life (21 min), to achieve anti-oxidant effect, following administration of APAP one log greater dose of 20 mg/kg was employed to achieve a robust antioxidant effect. Mice were euthanized at 4 h or 12 h. Livers were dissected, stored in 10% formalin, RNAlater and at −80 °C.

2.6. Liver enzymes test

Blood was collected under anaesthesia via retro orbital sinus

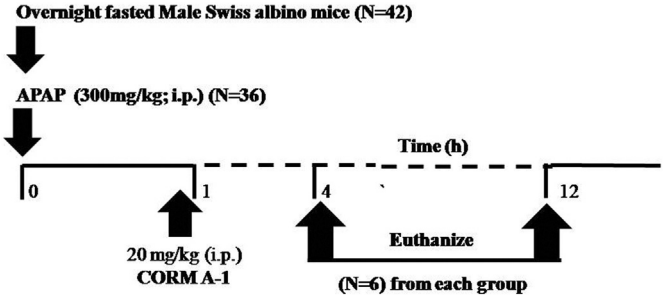

Fig. 1. Study design depicting treatment schedule of swiss albino male mice injected intraperitoneally with APAP (300 mg/kg). CORM A-1 (20 mg/kg, i.p) was injected after 1 h. Experimental groups include control, APAP treated or APAP + CORM-A1 treated mice ($n = 6$/group). Mice were euthanized at 4 and12 h followed by liver autopsy.

puncture. Serum was separated in a cold centrifuge at 3000 rpm for 15 min, and AST, ALT and ALP activity levels were estimated using Reckon Diagnostic kits (Vadodara, Gujarat, India).

2.7. Liver histopathology

Formalin-fixed livers ($n = 6$) were dehydrated, embedded in paraffin blocks and cut into 5-μm sections. The liver sections were stained with hematoxylin and eosin (H&E), photographed (Leica DM 2000 microscope), and scored for hepatocyte necrosis and vacuolation using semi-quantitative method (0, none; 1, < 10% of the total area; 2, < 30% of the total area; 3, < 50% of the total area; 4, > 50% of the total area) (Gujral et al., 2002) by two investigators blinded to the study.

2.8. Survival studies

Mice ($n = 30$) were divided into three groups ($n = 10$ each) i.e., control, APAP-acute dose (600 mg/kg) and APAP + CORM A-1-treated; CORM A-1 (20 mg/kg i.p.) was administered after 1 h of APAP injection. After APAP injection mice had free access to food and were observed every 1 h for initial 12 h. Subsequently (12–24 h), mice were observed every 4 h. Cumulative survival was plotted using Kaplan-Meier curves (GraphPad Prism 5.0Software, San Diego, CA).

2.9. GSH measurement

GSH was estimated in both HepG2 cells and mouse livers. After preparing 10% (*w/v*) liver homogenate, cellular debris was removed by centrifugation (650 *g* for 10 min at 4 °C) and protein content was quantified using Bradford reagent (BIO-RAD CA, USA). Reduced glutathione (GSH) was measured spectrophotometrically at 412 nm by assessing reduction of DTNB (dithiobis-2-nitrobenzoic acid) to a yellow anion. The GSH content was calculated as μg/mg protein using a standard GSH curve.

2.10. Quantitative real-time polymerase chain reaction (qPCR)

Total RNA was isolated from HepG2 cells and liver tissue samples using TRIzol reagent, and cDNA was synthesized using iScript cDNA Synthesis kit (BIO-RAD CA, USA). The mRNA levels of various genes were quantified by qPCR analysis (QuantStudio 12 K Flex, Life Technologies, CA, USA) using SYBR Select Master Mix. The data were normalized to GAPDH and analyzed using $2^{-\Delta\Delta CT}$ method (Schmittgen and Livak, 2008). Primers used for this study are listed in supplementary Table 1.

2.11. Immunoblot analyses

HepG2 cells were treated with CORM A-1 (100 μM) for 0, 30, 60, 120 min. Also, autopsy of liver from control and experimental groups of mice were collected and stored in liquid nitrogen. Both were separately homogenized with ice-cold lysis buffer. Nuclear proteins were isolated as described in NE-PER nuclear extraction kit (Thermo Scientific USA). Total proteins were quantified by Bradford assay wherein, equal amount (40 μg) was separated using 10% SDS gel electrophoresis. Protein was transferred to PVDF membranes (Bio-Rad, USA) and primary antibodies (1:500) for Nrf2 and HO-1 (1:1000) were added followed by secondary anti-rabbit horseradish peroxidase antibody (1:5000). Blots were developed using ECL reagent (Bio-Rad, Hercules, CA) and X-ray films. Anti-rabbit Lamin B and β-actin antibody (1:5000) were used to determine equivalent loading.

2.12. Molecular docking study

Molecular Docking of CO to Keap-1 was performed using open source software Auto Dock Vina (Trott and Olson, 2010). Cryo-crystallized structure of mouse Keap-1 was obtained from the protein data bank (PDB; 5CGJ) and binding mode of CO at the kelch domain of Keap-1 was investigated. Docking pose analysis was done with Discovery studio visualizer 4.5. These results were compared to a small molecule (3*S*)-1-[4-[(2,3,5,6-tetramethylphenyl) sulfonylamino]-1-naphthyl]pyrrolidine-3-carboxylic acid (RA839). All other docking parameters were default unless otherwise stated.

2.13. Statistical analysis

The data were expressed as mean ± SEM and analyzed by one-way analysis of variance (ANOVA), followed by Bonferroni's multiple comparison test using Graph Pad Prism 5.0 (CA, USA). $P < 0.05$ were considered significant.

3. Results

3.1. CORM A-1 attenuates t-BHP-induced oxidative stress and enhances HepG2 cell viability

We observed no cell death with CORM A-1 at doses as higher as 100 μM at 24 h (Fig. S1), further studies were performed using 100 μM CORM A-1. HepG2 cells treated with t-BHP (5, 10, 25, 50 μM) alone or with 100 μM CORM A-1, and cell viability was assessed by MTT assay. Fig. 2A indicates that t-BHP induced dose-dependent decrease in cell viability. At 2 h, 50 μM t-BHP induced 70% cell death. Addition of CORM A-1 (100 μM) significantly enhanced cell viability. t-BHP and CORM A-1 treated cells were also stained with DCFDA. Prominent fluorescence in t-BHP (25 and 50 μM)-treated cells indicated increased oxidative stress (Fig. 2B). However, t-BHP plus CORM A-1 treated cells had reduced fluorescence (2 fold at 25 μM and 1.5-fold at 50 μM) (Fig. 2C).

3.2. CORM A-1 modulates Nrf2 signaling in t-BHP-treated HepG2 cells

Expression of Nrf2 and its downstream target genes were studied in HepG2 cells. t-BHP-treated HepG2 cells had reduced mRNA levels of Nrf2, HO-1 and NQO1, and reduced GSH content. In contrast, co-treatment with CORM A-1 negated t-BHP-mediated effects significantly (Fig. 3 A-D) by enhancing Nrf2, HO-1 and NQO1 expression, and preventing GSH depletion.

3.3. CORM A-1 induced transcriptional activation of Nrf2

Transcriptional activation of Nrf2 was studied in the nuclear fraction of HepG2 cells. Immunoblot analysis of Nrf2 reveled a steady

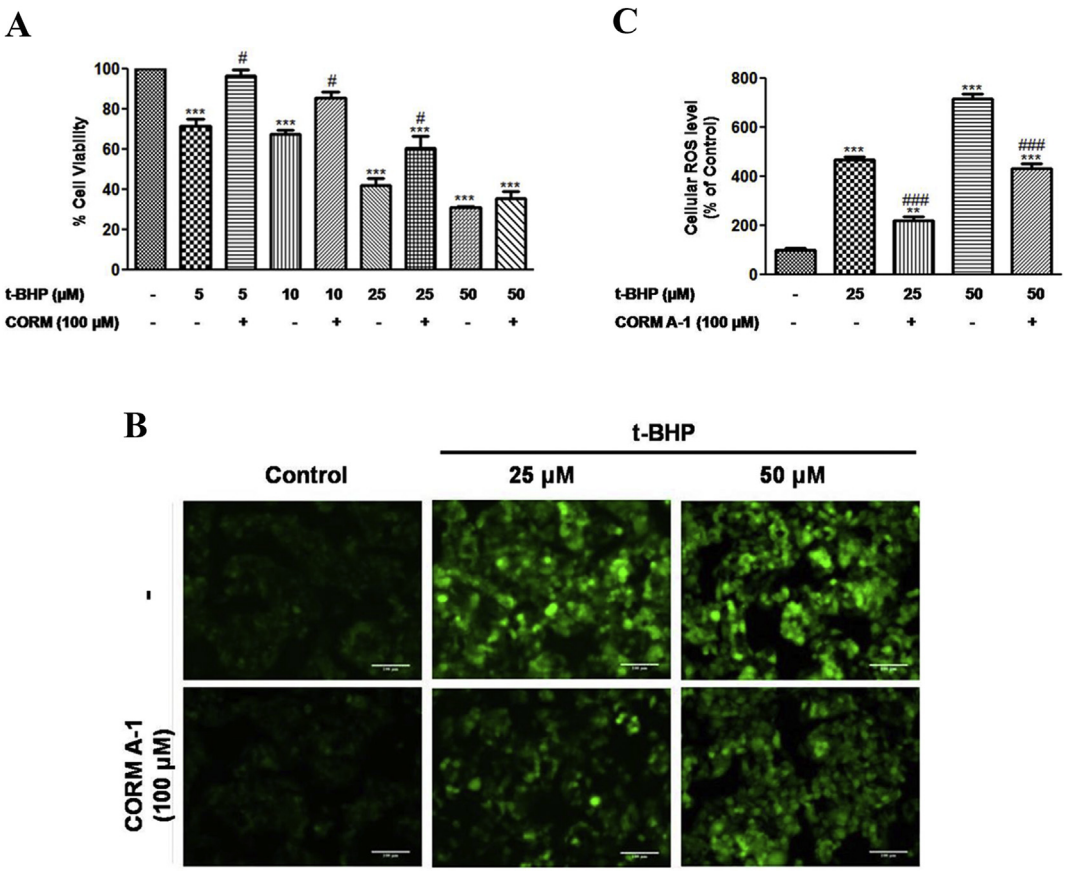

Fig. 2. HepG2 cells supplemented with CORM A-1 (100 μm) exposed to t-BHP (25 or 50 μm) for 2 h. (A) MTT assay (B) Intracellular ROS measurement using DCFDA staining (C) DCFDA stained images quantified using Image J software. Results expressed as Mean ± SEM. *P < 0.05, **P < 0.01 and ***P < 0.001 as compared to control group whereas; #P < 0.05, ##P < 0.01, and ###P < 0.001is when compared with respective t-BHP treated group ($n = 3$).

increment at 30, 60 and 120 min following CORM A-1 (100 μM) treatment. HO-1 is a key antioxidant gene that showed consistent upregulation at 60 and 120 min following CORM A-1 exposure (Fig. 4 A-B).

3.4. CORM A-1 reduces APAP-induced elevation of liver injury markers

APAP (300 mg/kg)-treated mice had significantly increased activity levels of serum AST, ALT and ALP at 4 and 12 h. In contrast, APAP-treated mice that received CORM A-1 (20 mg/kg) had reduced levels of AST, ALT and ALP (Fig. 5A-C).

3.5. CORM A-1 reduces APAP-induced hepatocyte necrosis

H&*E*-stained mouse liver sections were examined, scored and photographed (2.5× and 40×, Leica DMRB 2000). APAP-treated mice had focal necrosis, hepatocytes ballooning, nuclear condensation, sinusoidal enlargement, disruption of endothelial integrity and focalized fatty infiltration. At both 4 and 12 h, APAP-treated mice had increased hepatocytes necrosis (~1.5 fold) and vacuolation (~4 fold). Whereas, mice co-treated with CORM A-1 had reduced hepatocyte necrosis and vacuolation (~0.3 and ~1fold respectively) (Fig. 5D and F).

3.6. CORM A-1 improves survival of APAP-treated mice

Mice that received 600 mg/kg APAP (acute dose) were monitored for 24 h. Results are presented as Kaplan-Meier survival curves (Fig. 6). Compared to the control, APAP treatment induced 50% mortality ($n = 5$) by 4 h and 100% mortality by 10 h (additional 5). APAP + CORM A-1 treated mice had only 20% mortality ($n = 2$) by 4 h and 50% (additional 3) by the end of 6 h; thereafter no further mortality was recorded.

3.7. CORM A-1 facilitates Nrf2 translocation and activates ARE genes in APAP-treated mouse livers

To determine the antioxidant effects of CORM A-1, we assessed changes in hepatic expression of Nrf2 and ARE genes. Following APAP treatment, mRNA levels of Nrf2 were significantly decreased at 4 and 12 h. However, treatment with CORM A-1 abolished this effect (Fig. 7A, D, and F-H). Expression of Nrf2 protein in nuclear fraction confirms translocation at 4 and 12 h following CORM A-1 treatment. Compared to APAP-treated mice, those treated with CORM A-1, had enhanced mRNA and protein levels of HO-1. These results were further supported by an observed increment in mRNA of NQO-1 and GCLM, the downstream targets of Nrf2. In mice, treatment with APAP markedly reduced hepatic GSH. While, in those co-treated with CORM A-1, hepatic GSH content (Fig. 7I) was similar to untreated controls.

3.8. CORM A-1 alleviates APAP-induced upregulation of inflammatory cytokines

APAP-mediated sterile inflammation is initiated and perpetuated by damage-associated molecular patterns (DAMPs). We observed that in mice, treatment with APAP increased hepatic expression of both NF-κB and IL-1β, which were prevented by co-treatment with CORM A-1 (Fig. 8A-B). By 4 h, in the livers of APAP-treated mice, TNF-α levels were markedly increased; in mice treated with CORM A-1, hepatic TNF-α levels were significantly reduced. mRNA levels of IL-6 were not changed after APAP + CORM A-1 treated mice at both 4 and 12 h (Fig. 8C and D). Overall, these results indicate that treatment with

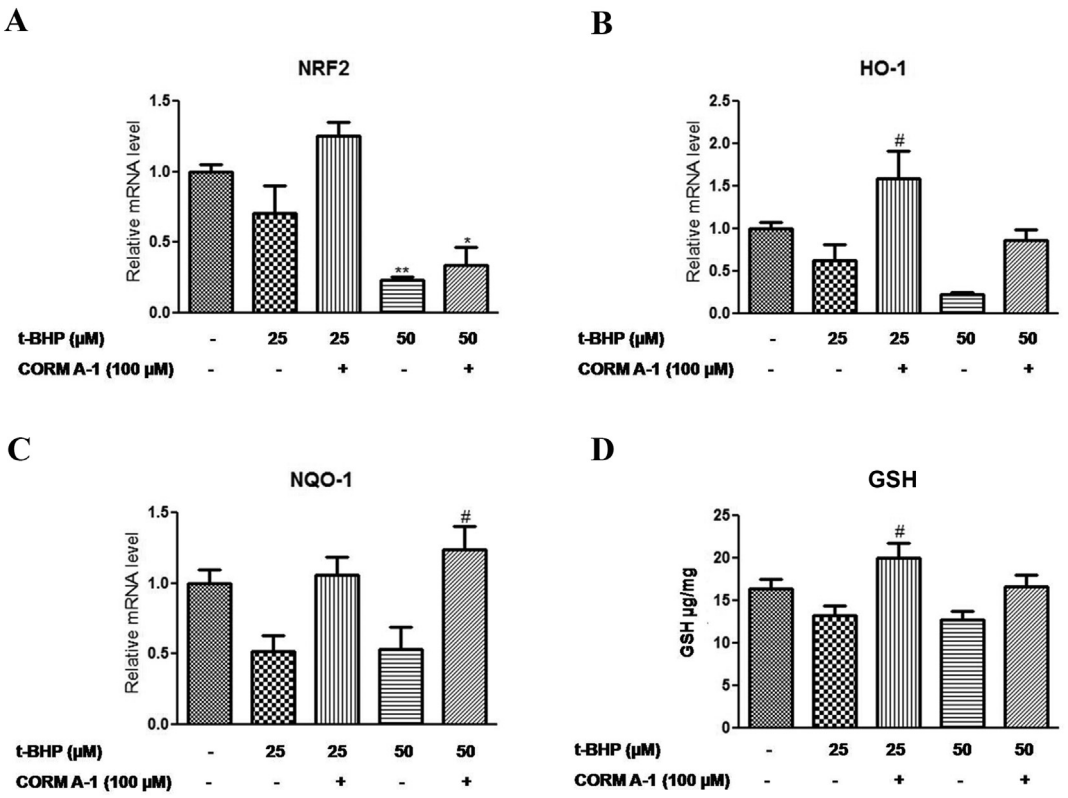

Fig. 3. HepG2 cells supplemented with CORM A-1 (100 μm) were exposed to t-BHP (25 μm) for 2 h. mRNA levels of Nrf2 and ARE related genes and, GSH content shown herein. (A) Nrf2 (B) HO-1 (C) NQO-1 (D) Total GSH level. Results expressed as Mean ± SEM. *P < 0.05, **P < 0.01 and *** P < 0.001 as compared to control group whereas; #P < 0.05, ##P < 0.01, and ###P < 0.001is when compared with respective t-BHP treated group (n = 3).

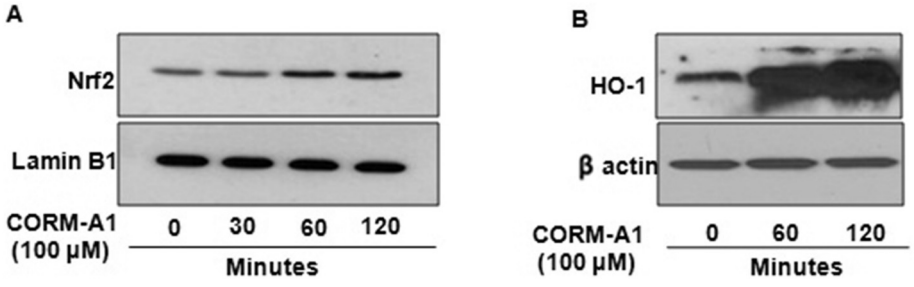

Fig. 4. Effect of CORM A-1 (100 μm) on Nrf2-ARE activation in HepG2 cells. Immunoblots of (A) Nrf2 (in nuclear fraction) and (B) HO-1(in cellular fraction) show that CORM A-1 inducts Nrf2 protein at 60 and 120 min. Correspondingly; HO-1 protein is also upregulated.

CORM A-1 reduces hepatic cytokine production, possibly via down-regulation of NF-κB, thus reducing the sterile inflammation.

3.9. CORM A-1 reduces Keap-1 expression and docks at Kelch domain

CORM A-1 releases CO in the medium and hence, docking interactions of CO with Keap-1 was analyzed (Fig. 9A-E) and the results were compared to a small molecule (3*S*)-1-[4-[(2,3,5,6-tetramethylphenyl) sulfonylamino]-1-naphthyl]pyrrolidine-3-carboxylic acid (RA839). RA839 is known to dock at kelch domain of Keap1 (5CGJ) thus inhibiting protein-protein interactions between Nrf2 and Keap-1 as evidenced by its crystal structure (Protein Data Bank - code 5CGJ) (Winkel et al., 2015). The binding energy of CO in a best pose was −1.6 kcal/mol. The ligand interaction analysis with Discovery studio Client demonstrated conventional hydrogen bond of carbon monoxide with VAL A: 606, GLY A: 367 and C—H bond with VAL A: 604, LEU A: 365 amino acids of Keap-1 protein. Comparative analysis of binding pattern with RA839 showed involvement of VAL A: 606 only. 3D visualization of CO binding on Keap-1 protein revealed that its binding location was at the base of Nrf2 binding pocket. CO binding induced changes in 3D configuration of Nrf2 binding pocket on Keap-1 protein leading to dissociation of Nrf2 and its possible activation.

4. Discussion

DILI-associated liver failure is related with oxidative stress-mediated hepatocyte death (Du et al., 2016; Ramachandran and Jaeschke, 2018). Herein, we investigated the therapeutic potential of CORM A-1, CO releasing molecule, in modulating oxidative stress-induced liver injury. In this regard, we utilized an in vitro model of oxidative stress and in vivo APAP induced acute liver injury in mouse. A recent study indicated that, CORM A-1 pre-treatment reduced Concanavalin A-induced hepatitis in mice (Mangano et al., 2018). In contrast, an important aspect of our experimental strategy was administration of CORM A-1 an hour *after* APAP overdose. This strategy was employed for various reasons. First, it mimicked the clinical scenarios wherein, patients seek care and are treated after the APAP overdose. Second, this strategy reduced the likelihood of interference with CYP450 activity

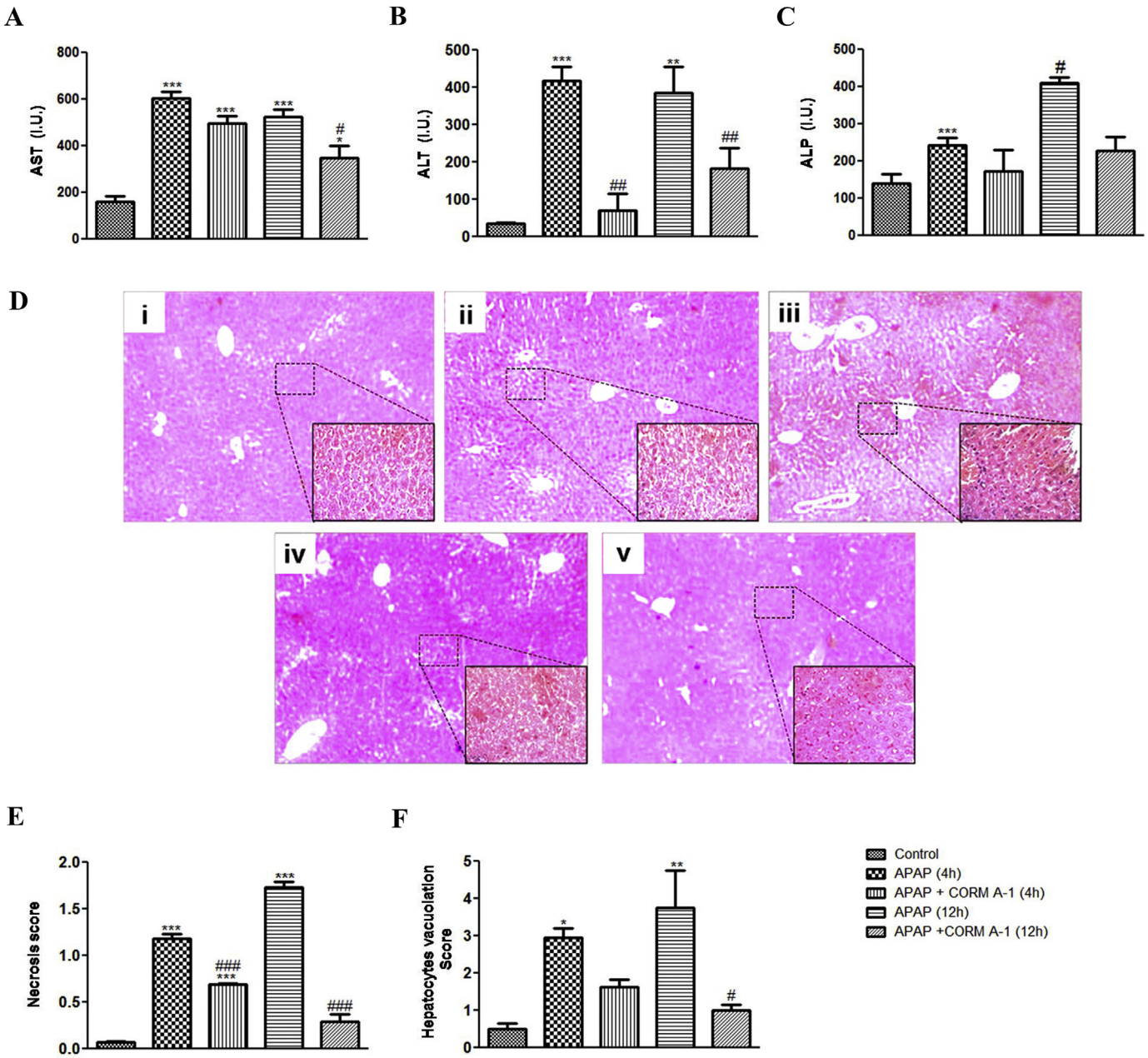

Fig. 5. Activity levels of marker enzymes of liver function in serum and microscopic evaluations of liver of control and treated mice. (A) AST, (B) ALT (C) ALP (D) H& *E*-stained liver sections (2.5× and insert 40×). Livers sections (3 per liver sample) scored for toxicity viz. (E) hepatocyte necrosis (F) hepatocyte vacuolation. CORM A-1 improved liver function and hepatocyte necrosis.

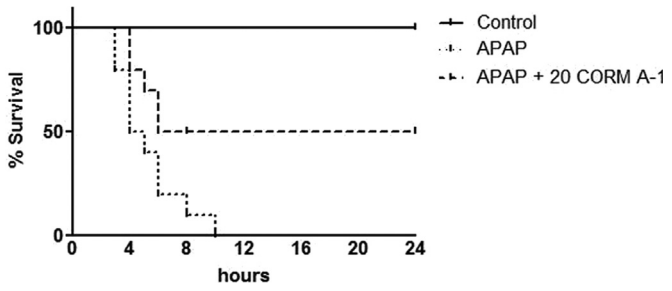

Fig. 6. Survival Study following lethal dose of APAP (600 mg/kg) and effect of CORM A-1 (20 mg/kg after 1 h). Experimental groups (n = 10 per group) included control, APAP treated or APAP + CORM A-1 treated mice. Kaplan–Meier survival curve shows improved survival in CORM A-1 treated mice.

(Du et al., 2015; Jadeja et al., 2015), since APAP is metabolized into NAPQI by CYP450, a critical step before the necrotic signaling is initiated. Third, NAPQI-mediated protein adduct formation is a key step in initiating hepatocyte necrosis (McGill et al., 2013). In mice, APAP-protein adduct formation peaks by 0.5–1 h and then declines thereafter along with GSH recovery(McGill et al., 2013). Administration of CORM A-1, 1 h after APAP overdose, prevented interference with this crucial signaling event. Collectively, these data suggest that CORM A-1 prevents liver injury by modulating late events such as induction of ARE genes and GSH recovery.

Previous studies had suggested that APAP-mediated liver injury is followed by sterile inflammation (Woolbright and Jaeschke, 2017). Other studies had indicated that IL-1β, TNF-α, and IL-6 are involved in liver regeneration (Jaeschke et al., 2012b; Bhushan et al., 2014). Also, role of inflammatory and immune cells in modulating APAP-mediated

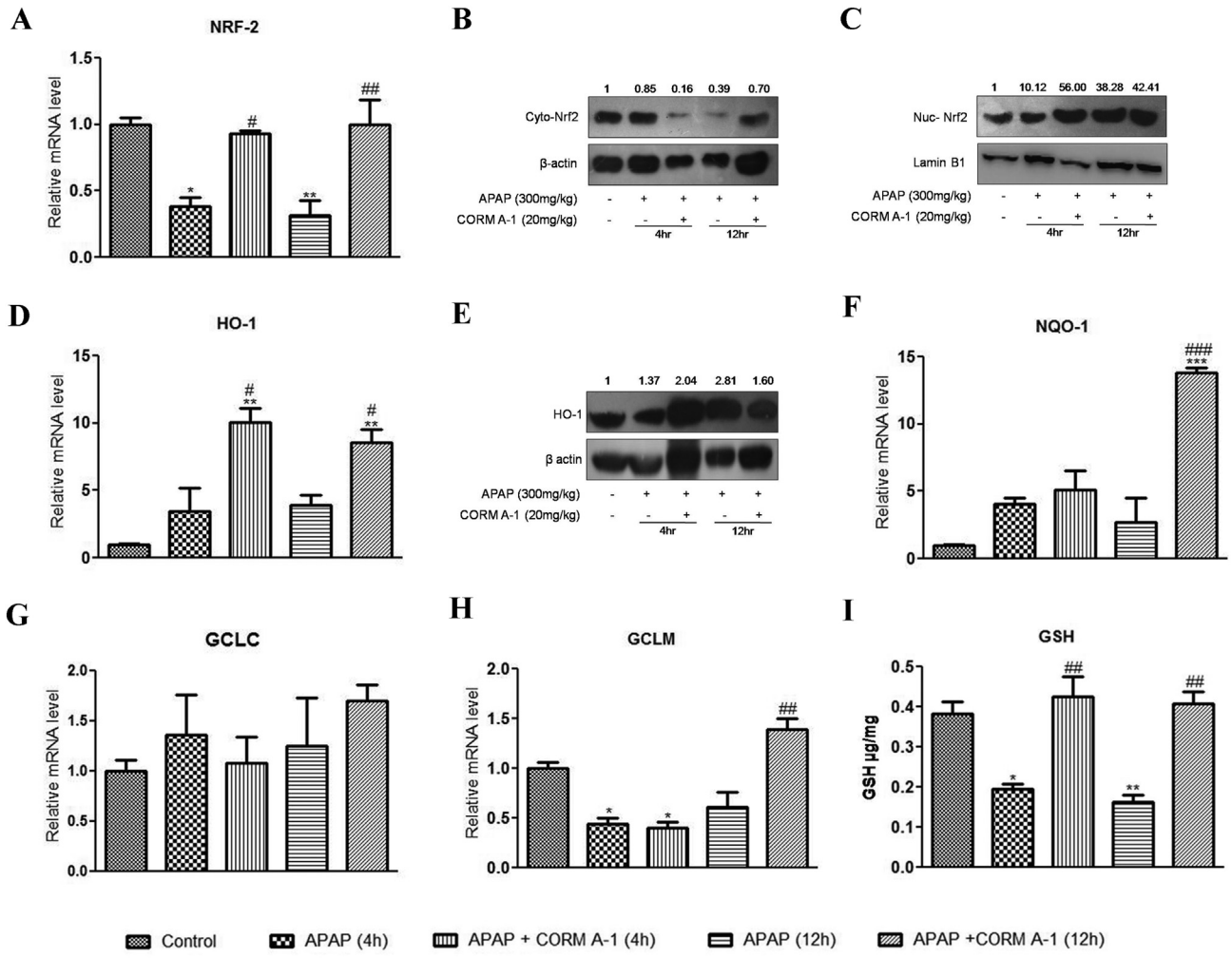

Fig. 7. mRNA levels of (A) Nrf2, (D) HO-1 (F) NQO-1, (G) GCLC (H) GCLM and (I) hepatic GSH content and immunoblots of (B) Nrf2 in cytosolic fraction, (C) Nrf2 in nuclear fraction and (E) HO-1 in cellular fraction of control and treated mice. Results expressed as Mean ± SEM. *P < 0.05, **P < 0.01 and *** P < 0.001 as compared to control group whereas; #P < 0.05, ##P < 0.01, and ###P < 0.001 is when compared with respective APAP treated group. CORM A-1 induced transcriptional activation of said genes that resulted in improvement in hepatic GSH.

liver injury is under active investigation wherein, NFκB upregulation and histoarchitectural changes are well-established (Ju, 2012; Barman et al., 2017). Lowered hepatic inflammation (reduced expression of NFκB, TNF-α and IL-1β) along with an improved functional status of liver observed in our study is comparable with hepatoprotection observed in APAP treated mice administered with saponin rich extract of *Rosa laevigata* michx fruit or Dioscin respectively (Zhao et al., 2012; Dong et al., 2014). However, by 12 h, while the TNF-α mRNA levels had reduced but were significant greater, more so in CORM A-1 co-treated mice, than untreated controls. Since APAP-treated mice that received CORM A-1 had less injury compared to those that did not, we think these effects to be secondary to reduced hepatocyte necrosis and generation of DAMPs.

Keap-1 is a substrate adaptor component in the Cullin3 (Cul3)-based ubiquitin E3 ligase complex, that recognizes Nrf2 by protein-protein interaction and negatively regulates Nrf2 by polyubiquitination (Jadeja et al., 2016b). Nuclear translocation of Nrf2 and regulatory role of Keap-1 has been emphasized in cellular anti-oxidant system by transcriptional activation of Nrf2-ARE genes. Our data regarding CORM A-1-induced upregulation of Nrf2 is similar to an effect seen in a mouse model of autoimmune hepatitis (Mangano et al., 2018) but its effect on Keap-1 lacked clarity. We observed that in APAP-treated mice, had reduced expression of Nrf2 that correlates with downregulation of Nrf2-ARE genes. On the other hand, APAP-treated mice that received CORM A-1 had higher levels of Nrf2 and HO-1 protein that lead to an increment in ARE related genes thus justifying the recorded improvement in hepatic GSH.

Currently NAC is the only FDA-approved antidote for APAP-induced hepatotoxicity. In humans, NAC is most effective when administrated within 8–10 h of APAP overdose (Lee et al., 2009). AASLD guidelines recommend NAC administration in all patients with suspected acute liver failure, irrespective of time of APAP ingestion (Ryter et al., 2006). Epidemiological studies indicate that within 4 days, most patients with APAP-induced liver either spontaneously recover, or die if not transplanted (Reddy et al., 2016). Since there is shortage of organs, and liver transplantation is either not feasible in many patients due to psychosocial reasons or not available in many centers across the world, for patients who present 10 h after APAP overdose, newer therapies are needed that promote liver regeneration. In case of a toxic insult, extending the therapeutic window is the key for an effective treatment (Carvalho et al., 2013) and, in our study, CORM A-1 was found to be effective even in the later stages accounting for an overall higher percentage survival.

NAC provides the necessary cysteine to enhance GSH synthesis and replete GSH stores(Rushworth and Megson, 2014; Khayyat et al., 2016). Our results suggest that CORM A-1 modulate later events such as GSH recovery and activation of ARE genes that enhance the anti-oxidant milieu of hepatocytes to promote recovery and provide

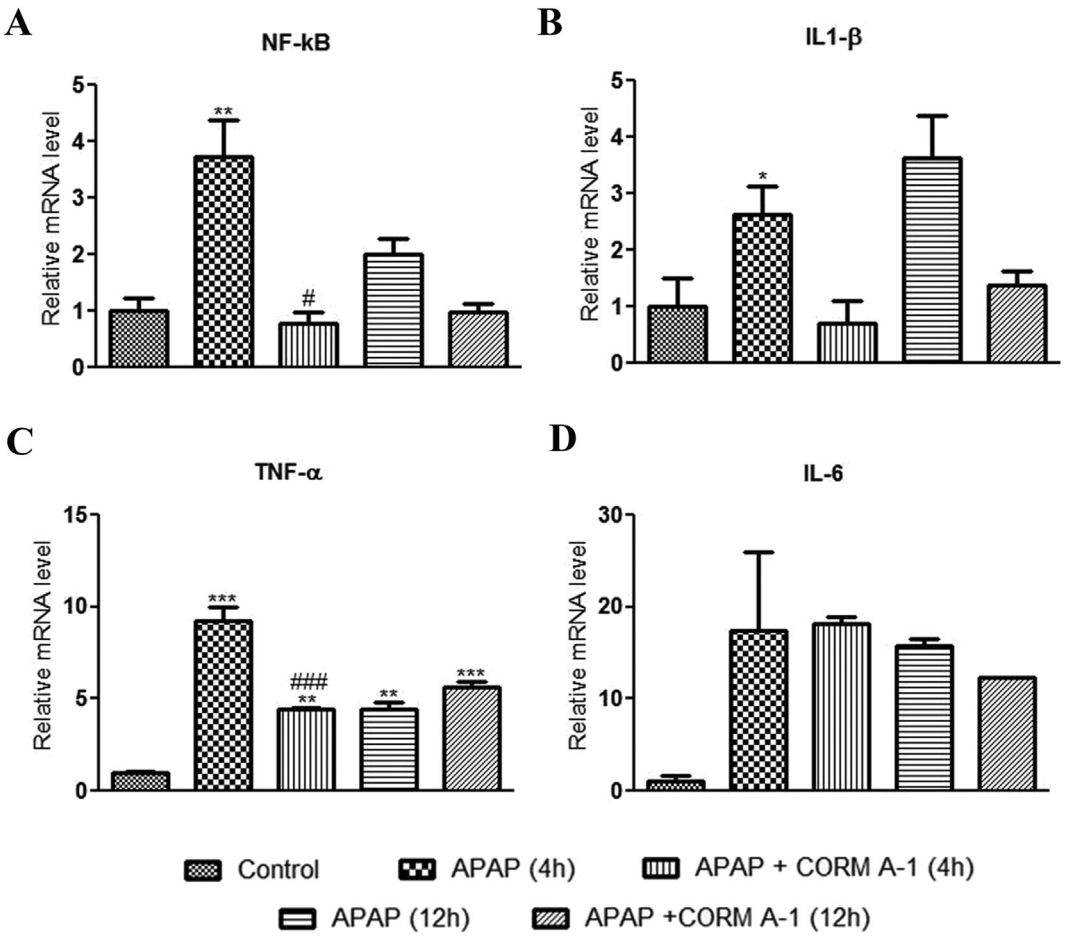

Fig. 8. mRNA levels of inflammatory marker genes (A) Nf-κB (B) IL-1β (C) TNF-α (D) IL-6 in liver of control and treated mice. Results expressed as Mean ± SEM. *P < 0.05, **P < 0.01 and *** P < 0.001 as compared to control group whereas; #P < 0.05, ##P < 0.01, and ###P < 0.001 is when compared with respective APAP treated group. CORM A-1 treatment caused lowered expression of said genes in liver.

hepatoprotection. Our in vitro findings corroborate in vivo data. Like most hepatocyte cell lines, HepG2 cells have inherently lower expression levels of CYP450 (Gerets et al., 2012). Therefore, here we used t-BHP, which is known to induce oxidative stress-mediated hepatocyte injury. CORM A-1-mediated reduction of t-BHP-induced oxidative stress and cellular injury suggests that CORM A-1 mediates it effects by reducing oxidative stress in hepatocytes. Previous studies had indicated that, in HepG2 cells, exogenous CO and tricarbonyl dichlororuthenium (II) dimer (RuCO; a CO releasing ligand), induces Nrf2 activation and increases transcription of HO-1(Lee et al., 2006). Immunoblots of nuc-Nrf2 envisaged herein implies towards an enhancement in CORM A-1 mediated nuclear translocation in HepG2 cells. Also, evidence of CORM A-1 mediated Nrf2 translocation was obtained in the immunoblot of APAP + CORM A-1 treated group. A concomitant increase recorded in immunoblot of HO-1 justifies Nrf2 mediated activation of ARE genes. These observations are also comparable to the reports on RuCO mediated Nrf2 activation. Due to their differences in chemical characteristics, RUCO is a faster releaser of CO (Lee et al., 2006) as compared to CORM A-1 that has a slow and sustained pattern of release (Motterlini et al., 2005). Hence, the CO mediated hepatoprotection observed herein is also attributable to the said chemical characteristics. Additionally, here we utilized a computational approach to determine the mechanism underlying CORM A-1-mediated Nrf2 activation. Our docking analysis indicated that CORM A-1 induced Nrf2 activation via CO-mediated release of Nrf2 from kelch domain of Keap-1. CORM A-1 is a slow releaser of CO. The molecular docking studies provide evidence that, the competitive binding of CO in kelch domain of Keap-1 inhibits interaction between Nrf2 and Keap-1. CO-Keap-1 interaction is assumed to stabilize the Keap-1 protein that facilitates release and activation of Nrf2 to induce ARE genes.

While the goal of this investigation was to determine the therapeutic potential of CORM A-1 in oxidative stress-mediated liver injury, some limitations need to be addressed in future. First, we studied the impact of CORM A-1 only at 4 and 12 h. This investigation does not address the impact on GSH decline and recovery in early phases of APAP-mediated liver injury. Second, these studies will need validation in mice with other genetic backgrounds. Previous studies had indicated that mice with different genetic background have variation in APAP metabolism, susceptibility to APAP-induced liver injury and patterns of serum ALT release.

In conclusion, these data indicate that CO releasing molecules reduce oxidative stress-mediated liver injury. The highlights of our study are **i)** in HepG2 cells, CORM A-1 facilitates nuclear translocation of Nrf 2, reduces oxidative stress, upregulates ARE genes, prevents GSH depletion and promotes cell viability; **ii)** in mice, CORM A-1 attenuates APAP-induced liver injury by induction of Nrf2 protein and ARE genes, preventing GSH depletion and by reducing hepatocyte necrosis; **iii)** in mice, CORM A-1 reduced APAP-induced mortality; **iv)** Docking analyses suggest that CORM A-1-mediated results are due to inhibition of interaction between Nrf2 and Keap-1. Collectively, therapeutic potential of CO releasing ligands in APAP-induced liver failure warrants further studies to understand its therapeutic potential in APAP-induced liver damage in humans.

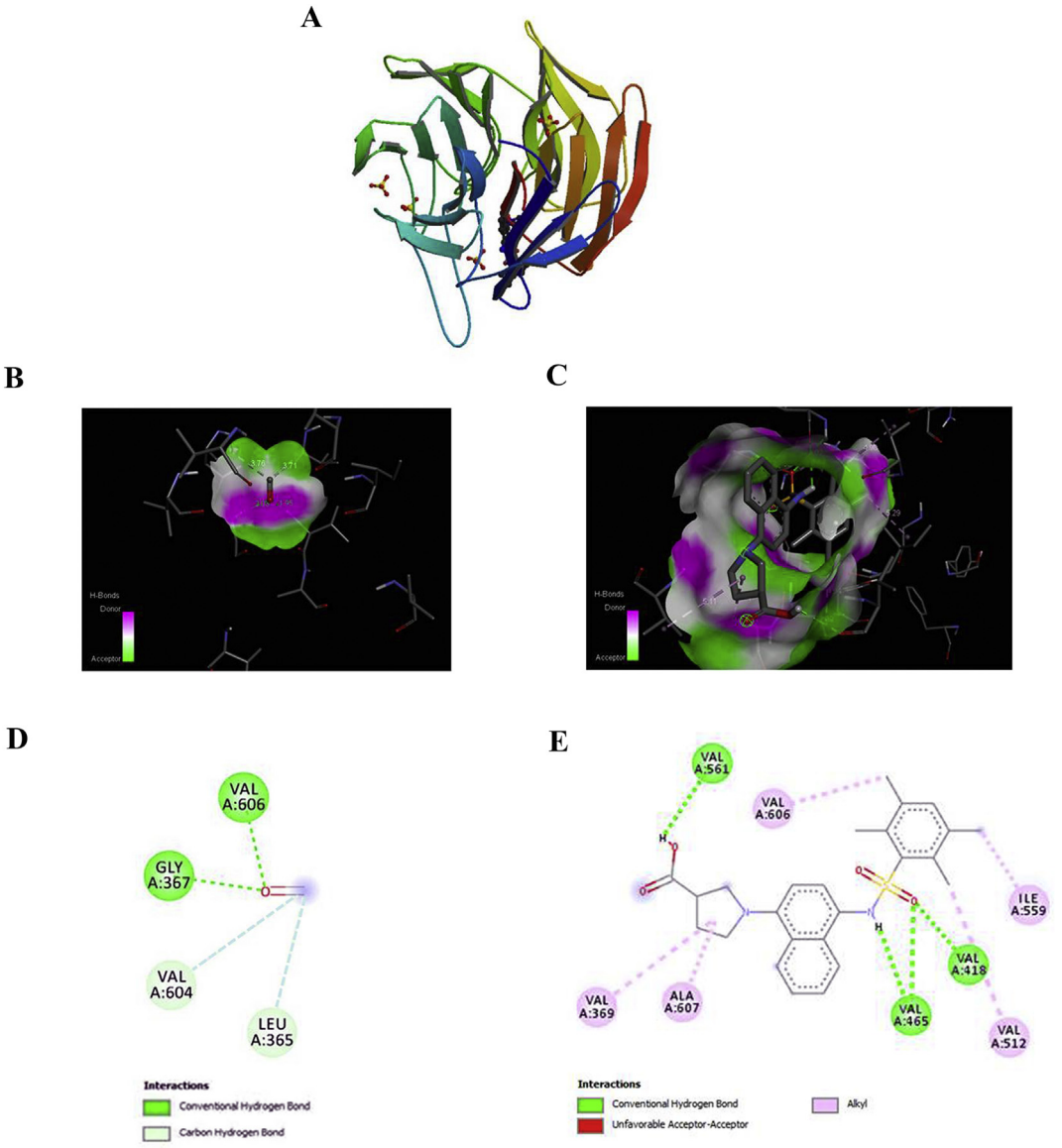

Fig. 9. Molecular docking analysis of CO with Keap1 Protein (A) Keap1 Protein PDB ID:5CGJ Crystal structure of murine Keap1 in complex with RA839, a non-covalent small-molecule binder to Keap1 and selective activator of Nrf2 signaling. (B) Top view of Keap1 in complex with CO (C) Top view of Keap1 in complex with RA839 (D) and (E) 2D interaction map of Keap1 with CO or RA839. The colour codes indicate potential interactions between amino acid residues and CO or RA839.

Conflict of interest

Authors have no conflict of interest.

Supplementary data to this article can be found online at https://doi.org/10.1016/j.taap.2018.09.034.

Acknowledgement

The author KKU is thankful to University Grant Commission for providing financial assistance in form of RFSMS fellowship F.25-1/2013-14(BSR)5-71/2007(BSR) Dt. 30/05/2014. This work was supported by Gujarat State Biotechnology Mission (GSBTM), Gandhinagar, Gujarat, India through MRP (GSBTM/MD/PROJECTS/SSA/4893/2016-17). Authors are also thankful to Prof. Rajesh Singh, Department of Biochemistry, MSU Baroda for extending real time thermal cycler facility and Dr. Kishore Rajput, Department of Botany, MSU Baroda for microscopy. Help rendered by Ms. Kavita Shirsath and Ms. Shweta Patel is also duly acknowledged.

References

Almeida, A.S., Soares, N.L., Vieira, M., Gramsbergen, J.B., Vieira, H.L., 2016. Carbon monoxide releasing molecule-A1 (CORM-A1) improves neurogenesis: increase of neuronal differentiation yield by preventing cell death. PLoS One 11, e0154781.

Barman, P., Mukherjee, R., Prusty, B., Suklabaidya, S., Senapati, S., Ravindran, B., 2017. Chitohexaose protects against acetaminophen-induced hepatotoxicity in mice. Cell Death Dis. 7, e2224.

Bhushan, B., Walesky, C., Manley, M., Gallagher, T., Borude, P., Edwards, G., Monga, S.P., Apte, U., 2014. Pro-regenerative signaling after acetaminophen-induced acute liver injury in mice identified using a novel incremental dose model. Am. J. Pathol. 184, 3013–3025.

Boczkowski, J., Poderoso, J.J., Motterlini, R., 2006. CO–metal interaction: vital signaling from a lethal gas. Trends Biochem. Sci. 31, 614–621.

Carvalho, N.R., da Rosa, E.F., da Silva, M.H., Tassi, C.C., Dalla Corte, C.L., Carbajo-Pescador, S., Mauriz, J.L., González-Gallego, J., Soares, F.A., 2013. New therapeutic approach: diphenyl diselenide reduces mitochondrial dysfunction in acetaminophen-induced acute liver failure. PLoS One 8, e81961.

ClinicalTrials.gov., Theatr. Record, 2015a. Carbon monoxide therapy for severe pulmonary arterial Hypertension (CO in PAH). Identifier: NCT01523548 First received: January 27, 2012; Last updated: April 1, 2015; Last verified: April 2015.

ClinicalTrials.gov., Theatr. Record, 2015b. Carbon monoxide to prevent Lung Inflammation Identifier. NCT00094406 First received: October 16, 2004; Last updated: May 20, 2015; Last verified: May 2015.

ClinicalTrials.gov., Theatr. Record, 2015c. Safety study of inhaled Carbon monoxide to treat acute respiratory distress syndrome (ARDS). Identifier: NCT02425579 First

received: March 17, 2015; Last updated: August 21, 2015; Last verified: August 2015.
ClinicalTrials.gov., Theatr. Record, 2015d. Study of inhaled Carbon monoxide to treat idiopathic pulmonary fibrosis. Identifier: NCT01214187. First received: September 30, 2010; Last updated: May 11, 2015; Last verified: May 2015.
Dong, D., Xu, L., Han, X., Qi, Y., Xu, Y., Yin, L., Liu, K., Peng, J., 2014. Effects of the total saponins from Rosa laevigata Michx fruit against acetaminophen-induced liver damage in mice via induction of autophagy and suppression of inflammation and apoptosis. Molecules 19, 7189–7206.
Du, K., McGill, M.R., Xie, Y., Bajt, M.L., Jaeschke, H., 2015. Resveratrol prevents protein nitration and release of endonucleases from mitochondria during acetaminophen hepatotoxicity. Food Chem. Toxicol. 81, 62–70.
Du, K., Ramachandran, A., Jaeschke, H., 2016. Oxidative stress during acetaminophen hepatotoxicity: sources, pathophysiological role and therapeutic potential. Redox Biol. 10, 148–156.
Espinosa-Diez, C., Miguel, V., Mennerich, D., Kietzmann, T., Sánchez-Pérez, P., Cadenas, S., Lamas, S., 2015. Antioxidant responses and cellular adjustments to oxidative stress. Redox Biol. 6, 183–197.
Fagone, P., Mangano, K., Mammana, S., Cavalli, E., Di Marco, R., Barcellona, M.L., Salvatorelli, L., Magro, G., Nicoletti, F., 2015. Carbon monoxide-releasing molecule-A1 (CORM-A1) improves clinical signs of experimental autoimmune uveoretinitis (EAU) in rats. Clin. Immunol. 157, 198–204.
Gerets, H., Tilmant, K., Gerin, B., Chanteux, H., Depelchin, B., Dhalluin, S., Atienzar, F., 2012. Characterization of primary human hepatocytes, HepG2 cells, and HepaRG cells at the mRNA level and CYP activity in response to inducers and their predictivity for the detection of human hepatotoxins. Cell Biol. Toxicol. 28, 69–87.
Gujral, J.S., Knight, T.R., Farhood, A., Bajt, M.L., Jaeschke, H., 2002. Mode of cell death after acetaminophen overdose in mice: apoptosis or oncotic necrosis? Toxicol. Sci. 67, 322–328.
Heard, K., Green, J., 2012. Acetylcysteine therapy for acetaminophen poisoning. Curr. Pharm. Biotechnol. 13, 1917–1923.
Hosick, P.A., Alamodi, A.A., Storm, M.V., Gousset, M.U., Pruett, B.E., Gray III, W., Stout, J., Stec, D.E., 2014. Chronic carbon monoxide treatment attenuates development of obesity and remodels adipocytes in mice fed a high-fat diet. Int. J. Obes. 38, 132–139.
Iwakiri, Y., Kim, M.Y., 2015. Nitric oxide in liver diseases. Trends Pharmacol. Sci. 36, 524–536.
Jadeja, R.N., Urrunaga, N.H., Dash, S., Khurana, S., Saxena, N.K., 2015. Withaferin-a reduces acetaminophen-induced liver injury in mice. Biochem. Pharmacol. 97, 122–132.
Jadeja, R.N., Upadhyay, K.K., Devkar, R.V., Khurana, S., 2016a. Naturally occurring Nrf2 activators: potential in treatment of liver injury. Oxidative Med. Cell. Longev. 2016, 3453926.
Jadeja, R.N., Upadhyay, K.K., Devkar, R.V., Khurana, S., 2016b. Naturally occurring Nrf2 activators: potential in treatment of liver injury. Oxidative Med. Cell. Longev. 2016, 3453926.
Jaeschke, H., McGill, M.R., Ramachandran, A., 2012a. Oxidant stress, mitochondria, and cell death mechanisms in drug-induced liver injury: lessons learned from acetaminophen hepatotoxicity. Drug Metab. Rev. 44, 88–106.
Jaeschke, H., Williams, C.D., Ramachandran, A., Bajt, M.L., 2012b. Acetaminophen hepatotoxicity and repair: the role of sterile inflammation and innate immunity. Liver Int. 32, 8–20.
James, L.P., McCullough, S.S., Lamps, L.W., Hinson, J.A., 2003. Effect of N-acetylcysteine on acetaminophen toxicity in mice: relationship to reactive nitrogen and cytokine formation. Toxicol. Sci. 75, 458–467.
Ju, C., 2012. Damage-associated molecular patterns: their impact on the liver and beyond during acetaminophen overdose. Hepatology 56, 1599–1601.
Kay, H.Y., Kim, Y.W., Ryu, D.H., Sung, S.H., Hwang, S.J., Kim, S.G., 2011. Nrf2-mediated liver protection by sauchinone, an antioxidant lignan, from acetaminophen toxicity through the PKCδ-GSK3β pathway. Br. J. Pharmacol. 163, 1653–1665.
Kerr, F., Dawson, A., Whyte, I.M., Buckley, N., Murray, L., Graudins, A., Chan, B., Trudinger, B., 2005. The Australasian Clinical Toxicology investigators Collaboration randomized trial of different loading infusion rates of N-acetylcysteine. Ann. Emerg. Med. 45, 402–408.
Khayyat, A., Tobwala, S., Hart, M., Ercal, N., 2016. N-acetylcysteine amide, a promising antidote for acetaminophen toxicity. Toxicol. Lett. 241, 133–142.
Knight, T.R., Ho, Y.-S., Farhood, A., Jaeschke, H., 2002. Peroxynitrite is a critical mediator of acetaminophen hepatotoxicity in murine livers: protection by glutathione. J. Pharmacol. Exp. Ther. 303, 468–475.
Lee, B.-S., Heo, J., Kim, Y.-M., Shim, S.M., Pae, H.-O., Kim, Y.-M., Chung, H.-T., 2006. Carbon monoxide mediates heme oxygenase 1 induction via Nrf2 activation in hepatoma cells. Biochem. Biophys. Res. Commun. 343, 965–972.
Lee, W.M., Hynan, L.S., Rossaro, L., Fontana, R.J., Stravitz, R.T., Larson, A.M., Davern, T.J., Murray, N.G., McCashland, T., Reisch, J.S., 2009. Intravenous N-acetylcysteine improves transplant-free survival in early stage non-acetaminophen acute liver failure. Gastroenterology 137, 856–864.
Liu, J., Li, C., Waalkes, M.P., Clark, J., Myers, P., Saavedra, J.E., Keefer, L.K., 2003. The nitric oxide donor, V-PYRRO/NO, protects against acetaminophen-induced hepatotoxicity in mice. Hepatology 37, 324–333.
Liu, W., Wang, D., Liu, K., Sun, X., 2012. Nrf2 as a converging node for cellular signaling pathways of gasotransmitters. Med. Hypotheses 79, 308–310.
Mangano, K., Cavalli, E., Mammana, S., Basile, M.S., Caltabiano, R., Pesce, A., Puleo, S., Atanasov, A.G., Magro, G., Nicoletti, F., 2018. Involvement of the Nrf2/HO-1/CO axis and therapeutic intervention with the CO-releasing molecule CORM-A1, in a murine model of autoimmune hepatitis. J. Cell. Physiol. 233, 4156–4165.
Mani, M., Khaghani, S., Mohammadi, T.G., Zamani, Z., Azadmanesh, K., Meshkani, R., Pasalar, P., Mostafavi, E., 2013. Activation of Nrf2-antioxidant response element mediated glutamate cysteine ligase expression in hepatoma cell line by homocysteine. Hepat. Mon. 13, e8394.
McGill, M.R., Lebofsky, M., Norris, H.-R.K., Slawson, M.H., Bajt, M.L., Xie, Y., Williams, C.D., Wilkins, D.G., Rollins, D.E., Jaeschke, H., 2013. Plasma and liver acetaminophen-protein adduct levels in mice after acetaminophen treatment: dose–response, mechanisms, and clinical implications. Toxicol. Appl. Pharmacol. 269, 240–249.
Morsy, M.A., Ibrahim, S.A., Abdelwahab, S.A., Zedan, M.Z., Elbitar, H.I., 2010. Curative effects of hydrogen sulfide against acetaminophen-induced hepatotoxicity in mice. Life Sci. 87, 692–698.
Motterlini, R., Otterbein, L.E., 2010. The therapeutic potential of carbon monoxide. Nat. Rev. Drug Discov. 9, 728–749.
Motterlini, R., Clark, J.E., Foresti, R., Sarathchandra, P., Mann, B.E., Green, C.J., 2002. Carbon monoxide-releasing molecules: characterization of biochemical and vascular activities. Circ. Res. 90, e17–e24.
Motterlini, R., Mann, B.E., Johnson, T.R., Clark, J.E., Foresti, R., Green, C.J., 2003. Bioactivity and pharmacological actions of carbon monoxide-releasing molecules. Curr. Pharm. Des. 9, 2525–2539.
Motterlini, R., Sawle, P., Hammad, J., Bains, S., Alberto, R., Foresti, R., Green, C., 2005. CORM-A1: a new pharmacologically active carbon monoxide-releasing molecule. FASEB J. 19, 284–286.
Network, T.I., 2010. A multicenter comparison of the safety of oral versus intravenous acetylcysteine for treatment of acetaminophen overdose. Clin. Toxicol. 48, 424–430.
Nikolic, I., Saksida, T., Mangano, K., Vujicic, M., Stojanovic, I., Nicoletti, F., Stosic-Grujicic, S., 2014. Pharmacological application of carbon monoxide ameliorates islet-directed autoimmunity in mice via anti-inflammatory and anti-apoptotic effects. Diabetologia 57, 980–990.
Nikolic, I., Saksida, T., Vujicic, M., Stojanovic, I., Stosic-Grujicic, S., 2015. Anti-diabetic actions of carbon monoxide-releasing molecule (CORM)-A1: Immunomodulation and regeneration of islet beta cells. Immunol. Lett. 165, 39–46.
Nourjah, P., Ahmad, S.R., Karwoski, C., Willy, M., 2006. Estimates of acetaminophen (paracetomal)-associated overdoses in the United States. Pharmacoepidemiol. Drug Saf. 15, 398–405.
Otterbein, L.E., Bach, F.H., Alam, J., Soares, M., Lu, H.T., Wysk, M., Davis, R.J., Flavell, R.A., Choi, A.M., 2000. Carbon monoxide has anti-inflammatory effects involving the mitogen-activated protein kinase pathway. Nat. Med. 6, 422–428.
Ramachandran, A., Jaeschke, H., 2018. Oxidative stress and acute hepatic injury. Curr. Opin. Toxicol. 7, 17–21.
Reddy, K.R., Ellerbe, C., Schilsky, M., Stravitz, R.T., Fontana, R.J., Durkalski, V., Lee, W.M., 2016. Determinants of outcome among patients with acute liver failure listed for liver transplantation in the United States. Liver Transpl. 22, 505–515.
Rushworth, G.F., Megson, I.L., 2014. Existing and potential therapeutic uses for N-acetylcysteine: the need for conversion to intracellular glutathione for antioxidant benefits. Pharmacol. Ther. 141, 150–159.
Ryter, S.W., Alam, J., Choi, A.M., 2006. Heme oxygenase-1/carbon monoxide: from basic science to therapeutic applications. Physiol. Rev. 86, 583–650.
Saito, C., Lemasters, J.J., Jaeschke, H., 2010. C-Jun N-terminal kinase modulates oxidant stress and peroxynitrite formation independent of inducible nitric oxide synthase in acetaminophen hepatotoxicity. Toxicol. Appl. Pharmacol. 246, 8–17.
Schmittgen, T.D., Livak, K.J., 2008. Analyzing real-time PCR data by the comparative C(T) method. Nat. Protoc. 3, 1101–1108.
Trott, O., Olson, A.J., 2010. AutoDock Vina: improving the speed and accuracy of docking with a new scoring function, efficient optimization and multithreading. J Comput Chem 31, 455–461.
Urquhart, P., Rosignoli, G., Cooper, D., Motterlini, R., Perretti, M., 2007. Carbon monoxide-releasing molecules modulate leukocyte-endothelial interactions under flow. J. Pharmacol. Exp. Ther. 321, 656–662.
Urrunaga, N.H., Jadeja, R.N., Rachakonda, V., Ahmad, D., McLean, L.P., Cheng, K., Shah, V., Twaddell, W.S., Raufman, J.-P., Khurana, S., 2015. M1 muscarinic receptors modify oxidative stress response to acetaminophen-induced acute liver injury. Free Radic. Biol. Med. 78, 66–81.
Varadi, J., Lekli, I., Juhasz, B., Bacskay, I., Szabo, G., Gesztelyi, R., Szendrei, L., Varga, E., Bak, I., Foresti, R., 2007. Beneficial effects of carbon monoxide-releasing molecules on post-ischemic myocardial recovery. Life Sci. 80, 1619–1626.
Whyte, I.M., Francis, B., Dawson, A.H., 2007. Safety and efficacy of intravenous N-acetylcysteine for acetaminophen overdose: analysis of the Hunter Area Toxicology Service (HATS) database. Curr. Med. Res. Opin. 23, 2359–2368.
Winkel, A.F., Engel, C.K., Margerie, D., Kannt, A., Szillat, H., Glombik, H., Kallus, C., Ruf, S., Güssregen, S., Riedel, J., 2015. Characterization of RA839, a noncovalent small molecule binder to Keap1 and selective activator of Nrf2 signaling. J. Biol. Chem. 290, 28446–28455.
Woolbright, B.L., Jaeschke, H., 2017. The impact of sterile inflammation in acute liver injury. J. Clin. Transl. Res. 3, 157–169.
Yan, F., Zhang, Q.-Y., Jiao, L., Han, T., Zhang, H., Qin, L.-P., Khalid, R., 2009. Synergistic hepatoprotective effect of Schisandrae lignans with Astragalus polysaccharides on chronic liver injury in rats. Phytomedicine 16, 805–813.
Zhang, X., Shan, P., Alam, J., Fu, X.-Y., Lee, P.J., 2004. Carbon monoxide differentially modulates STAT1 and STAT3 and inhibits apoptosis via a PI3K/Akt and p38 kinase-dependent STAT3 pathway during anoxia-reoxygenation injury. J. Biol. Chem. 280, 8714–8721.
Zhang, Q.-Y., Chu, X.-Y., Jiang, L.-H., Liu, M.-Y., Mei, Z.-L., Zhang, H.-Y., 2017. Identification of non-electrophilic Nrf2 activators from approved drugs. Molecules 22, 1–12.
Zhao, X., Cong, X., Zheng, L., Xu, L., Yin, L., Peng, J., 2012. Dioscin, a natural steroid saponin, shows remarkable protective effect against acetaminophen-induced liver damage in vitro and in vivo. Toxicol. Lett. 214, 69–80.
Zhu, R., Wang, Y., Zhang, L., Guo, Q., 2012. Oxidative stress and liver disease. Hepatol. Res. 42, 741–749.

Redox Biology 28 (2020) 101314

Contents lists available at ScienceDirect

Redox Biology

journal homepage: www.elsevier.com/locate/redox

Research Paper

Carbon monoxide releasing molecule-A1 improves nonalcoholic steatohepatitis via Nrf2 activation mediated improvement in oxidative stress and mitochondrial function

Kapil K. Upadhyay[a], Ravirajsinh N. Jadeja[b], Hitarthi S. Vyas[a], Bhaumik Pandya[c], Apeksha Joshi[a], Aliasgar Vohra[a], Menaka C. Thounaojam[d], Pamela M. Martin[b], Manuela Bartoli[d,**], Ranjitsinh V. Devkar[a,*]

[a] Metabolic Endocrinology Division, Department of Zoology, Faculty of Science, The Maharaja Sayajirao University of Baroda, Vadodara, Gujarat, 390002, India
[b] Department of Biochemistry and Molecular Biology, Augusta University, Augusta, GA, 30912, USA
[c] Georgia Cancer Center, Augusta University, Augusta, GA, 30912, USA
[d] Department of Ophthalmology, Medical College of Georgia, Augusta University, Augusta, GA, 30912, USA

ARTICLE INFO

Keywords:
CORM-A1
NASH
Nrf2
Mitochondria
ROS

ABSTRACT

Nuclear factor-erythroid 2 related factor 2 (Nrf2)-mediated signaling plays a central role in maintaining cellular redox homeostasis of hepatic cells. Carbon monoxide releasing molecule-A1 (CORM-A1) has been reported to stimulate up-regulation and nuclear translocation of Nrf2 in hepatocytes. However, the role of CORM-A1 in improving lipid metabolism, antioxidant signaling and mitochondrial functions in nonalcoholic steatohepatitis (NASH) is unknown. In this study, we report that CORM-A1 prevents hepatic steatosis in high fat high fructose (HFHF) diet fed C57BL/6J mice, used as model of NASH. The beneficial effects of CORM-A1 in HFHF fed mice was associated with improved lipid homeostasis, Nrf2 activation, upregulation of antioxidant responsive (ARE) genes and increased ATP production. As, mitochondria are intracellular source of reactive oxygen species (ROS) and important sites of lipid metabolism, we further investigated the mechanisms of action of CORM-A1-mediated improvement in mitochondrial function in palmitic acid (PA) treated HepG2 cells. Cellular oxidative stress and cell viability were found to be improved in PA + CORM-A1 treated cells via Nrf2 translocation and activation of cytoprotective genes. Furthermore, in PA treated cells, CORM-A1 improved mitochondrial oxidative stress, membrane potential and rescued mitochondrial biogenesis thru upregulation of Drp1, TFAM, PGC-1α and NRF-1 genes. CORM-A1 treatment improved cellular status by lowering glycolytic respiration and maximizing OCR. Improvement in mitochondrial respiration and increment in ATP production in PA + CORM-A1 treated cells further corroborate our findings. In summary, our data demonstrate for the first time that CORM-A1 ameliorates tissue damage in steatotic liver via Nrf2 activation and improved mitochondrial function, thus, suggesting the anti-NASH potential of CORM-A1.

1. Introduction

Multitude of metabolic diseases, including non-alcoholic steatohepatitis (NASH), have been implicated to higher consumption of fat-rich and high calorie foods [1]. About 15% of the total obese individuals with symptoms of metabolic syndrome constitute the high-risk group for NASH. Ethnicity, dietary habits, genetic and environmental factors further contribute towards the observed variations in occurrence of NASH [2,3]. Excess lipid accumulation in hepatocytes, high oxidative stress and inflammation are the key players in pathogenesis of NASH [4]. Currently used symptomatic treatment protocols for NASH include the lipid lowering, anti-diabetic, antioxidants or anti-inflammatory drugs coupled with changes in lifestyle. However, no FDA approved drug is presently available for this potentially lethal disease [5]. Patients with NASH develop anomalies in the ultrastructure of mitochondria, impairment of hepatic ATP synthesis and increased mitochondrial ROS production [6,7]. Lipid peroxidation, cytokine production and fatty manifestations in liver causes cell death and overall impairment of liver function [8].

The transcription factor nuclear factor erythroid 2-related factor 2

* Corresponding author.
** Corresponding author.
E-mail addresses: mbartoli@augusta.edu (M. Bartoli), rv.devkar-zoo@msubaroda.ac.in (R.V. Devkar).

https://doi.org/10.1016/j.redox.2019.101314
Received 12 July 2019; Received in revised form 27 August 2019; Accepted 30 August 2019
Available online 31 August 2019
2213-2317/ © 2019 The Authors. Published by Elsevier B.V. This is an open access article under the CC BY license (http://creativecommons.org/licenses/BY/4.0/).

(Nrf2) enables cell survival and adaptation under conditions of stress by regulating cytoprotective proteins, intracellular antioxidants, anti-inflammatory and detoxifying enzymes. In addition, Nrf2 also protects the liver against steatosis by restraining lipogenesis and by improving oxidation of unsaturated fats [9]. Therefore, a variety of Nrf2 activators such as phytochemicals, drugs or gasotransmitters have been investigated for their therapeutic potential in treating metabolic disorders [10–12].

Gasotransmitters (CO, H_2S and NO) are molecules that are naturally produced and degraded within the human body. In liver, carbon monoxide (CO) is produced endogenously by heme oxygenase (HO)-mediated degradation of heme. This process also yields free iron and biliverdin that is rapidly converted into the antioxidant bilirubin [13]. Unlike other gasotransmitters, CO is relatively stable and has affinity towards transitional metals [14]. High levels of CO have been detected in breath of asthmatic and diabetic patients that underwent decrement following steroid or insulin treatment [15,16]. CO has been implicated in regulating mitochondrial ROS, cytochrome c oxidase, oxygen consumption, oxidative metabolism and overall mitochondrial functioning [17]. CO is also known to have beneficial effects against inflammation and hemorrhagic shock [18,19]. CO-releasing molecules (CO-RMs), are classes of organometallic compounds that have been developed to mimic the antioxidant, anti-inflammatory and cytoprotective properties of CO by ensuring its sustained release in biological systems [20]. Carbon monoxide releasing molecule A-1 (CORM-A1) has a boron core and is reported for slow and sustained release of CO in living systems ($t_{1/2}$ = 21 min) [21]. Therapeutic effects of CORM-A1 in various diseases model such as diabetes, myocardial infarction and posterior uveitis is well established [22–24].

Reported attributes of CORM-A1 in alleviating oxidative stress and providing cytoprotection forms the basis of our hypothesis. Previous studies conducted in our lab had shown that CORM-A1 reduces oxidative stress in acetaminophen induced liver injury in mice via Nrf2 activation [25]. In this study, we had used *in vivo* and *in vitro* experimental models to evaluate the effects of CORM-A1 in improving various features associated with pathology of NASH i.e. hepatic steatosis, oxidative stress, inflammation and mitochondrial dysfunction.

2. Materials and methods

2.1. Chemical and reagents

Chemicals for cell culture like Dulbecco's modified eagle's medium (DMEM), fetal bovine serum (FBS), trypsin phosphate versene glucose (TPVG), bovine serum albumin (BSA) and antibiotic-antimycotic solution were purchased from Hi-media laboratories (Mumbai, India). TRIzol and SYBR select master mix were procured from Invitrogen (CA, USA). iScript cDNA synthesis kit was procured from Bio-Rad (CA, USA). Antibodies Nrf2 (12721S), HO-1 (70081S), β-actin (4970S) and 2° Antibody (7074P2) were purchased from cell signaling technology (Danvers, MA). PGC-1α (ab54481), Keap1 (ab139729), NRF-1 (ab175932) were purchased from Abcam (Cambridge, MA, USA). RNAlater stabilizing solution was purchased from Ambion Inc. (USA). CORM-A1, haematoxylin, eosin and palmitic acid (PA) were purchased from Sigma aldrich (St. Louis, MO, USA). Methanol, dimethyl sulphoxide (DMSO), 3-(4,5-dimethylthiazol-2-yl)-2,5-diphenyl tetrazolium bromide (MTT) were purchased from Sisco research laboratory Pvt. Ltd. (Mumbai, India).

2.2. Animal studies and experimental protocols

C57BL/6J male mice (6–8 weeks of age) were purchased from ACTREC Mumbai and maintained as per CPCSEA standard guidelines (23 ± 2 °C, LD 12:12, laboratory chow and water ad libitum) followed by a week-long acclimatization. Protocol was approved by Institutional Animal Ethical Committee (IAEC) (Approval no. MSU-Z/IAEC/02-2017) and experiments were conducted in CPCSEA approved animal house facility of Department of Zoology, The Maharaja Sayajirao University of Baroda, Vadodara, Gujarat, India (827/GO/Re/S/04/CPCSEA).

Mice were randomly divided into three groups with six animals per group. The entire period of experiment was of 16 weeks. Group I (SD) was fed with standard diet (SD). Group II (HFHF) was fed with high fat diet + 20% Fructose (HFHF diet) [26]. Group III (HFHF + CORM-A1) was fed with HFHF diet for 16 weeks and CORM-A1 was injected (ip:2 mg/kg/day) from 9th to 16th week. Food intake, water intake and body weights were recorded every week throughout the period of study. At the end of 16 weeks, animals were fasted overnight and whole blood was collected by retro-orbital sinus puncture under mild isoflurane anaesthesia. Whole blood was centrifuged (at 4 °C and 3000 rpm for 10 min) and serum was collected and stored. Later, mice were sacrificed, and liver and visceral fat were collected. These tissue samples were stored in 10% formalin (for histopathology), in RNAlater (for gene expression studies) or at −80°C (for protein analysis).

2.3. Serum biochemical parameters

Levels of circulating enzymes indicative of liver function (AST, ALT and ALP) and serum lipid profile (TL, TC, TG, LDL, VLDL, CHL/HDL and LDL/HDL ratio) were estimated using commercially available kits (Reckon Diagnostic kits, Vadodara, Gujarat, India).

2.4. Liver histopathology

Formalin fixed liver and adipose tissue (n = 6) were dehydrated and embedded in paraffin wax blocks and cut into 5 μm thick sections. These sections were stained with haematoxylin and eosin (H&E) and were observed and photographed (Leica DM 2500 microscope). Investigators blinded to this study conducted scoring of ballooning hepatocytes and steatotic liver sections of control and treated mice [27]. Adipose tissue sections were observed, photographed and morphometric scoring was done for the same.

2.5. Quantitative real-time polymerase chain reaction (qPCR) analysis

Total RNA content from control and treated liver and HepG2 cells was isolated using TRIzol reagent and cDNA was synthesized using iScript cDNA Synthesis kit (BIO-RAD CA, USA). mRNA levels of candidate genes (S. Table- 1) were quantified by qPCR analysis (QuantStudio-3 real time PCR, Life Technologies, CA, USA) using SYBR Select Master Mix. The data were normalized to the internal control GAPDH and analysed using $2^{-\Delta\Delta CT}$ method.

2.6. Immunoblot analysis

Control and treated liver samples and HepG2 cells were homogenized with ice-cold lysis buffer. Nuclear proteins were isolated as described in NE-PER nuclear extraction kit (Thermo Scientific USA). Total protein content was quantified by Bradford assay wherein, equal amount (40 μg) was separated using 10% SDS polyacrylamide gel electrophoresis. Proteins were transferred on to PVDF membrane (Bio-Rad, USA) and primary antibodies for Nrf2, HO-1, Keap1, NRF-1 or PGC 1-α (1:1000) were added followed by secondary anti-rabbit horseradish peroxidase antibody (1:5000). Blots were stripped using stripping buffer (Thermo Scientific, Wilmington, DE) and re-probed with goat anti-rabbit Lamin B and β-actin antibody (1:5000) to determine equivalent loading. Blots were developed using ECL reagent (Bio-Rad, Hercules, CA) and visualized in iBright Imaging System.

2.7. Co-immunoprecipitation assay

The interaction of Nrf2 with Keap1 following CORM-A1 treatment

to HepG2 cells was assayed by co-immunoprecipitation (co-IP) assay using magnetic beads according to the manufacturer's protocol (Pierce Classic Magnetic IP/Co-IP Kit). 500 μg of protein from different experimental groups was mixed with 10 μg Nrf2 antibody overnight at 4 °C to form the immune complex. 25 μl of pre-washed Pierce Protein A/G Magnetic Beads were placed into the above immune complex and incubated for 1 h with mixing. Then the beads were washed, and the target antigen was eluted with alternative elution method. Target antigen and the binding proteins were immunoblotted with the indicated antibodies by Western blot assay.

2.8. Mitochondrial DNA copy number

Mitochondrial DNA (mtDNA) was used to determine mitochondrial density using q-PCR. Briefly, total DNA was isolated from liver tissue or HepG2 cells using GeneJET genomic DNA purification kit (Thermo Scientific, USA) according to the manufacturer's instructions. The mtDNA copy number was calculated from the ratio of Cytochrome b (mitochondrial encoded gene) to Nuclear18s rRNA (nuclear-encoded gene).

2.9. Total ATP content

ATP content was determined using an ATP Determination Kit (A22066, Molecular Probes). Each reaction contained 1.25 μg/ml firefly luciferase, 0.5 mM D-luciferin and 1 mM dithiothreitol in 100 ml reaction buffer. At the end of each experiment, ATP content was measured in liver tissue. After 15-min incubation luminescence was measured in Synergy HTX Multimode Reader (Bio-Tek instruments, Inc., Winooski, VT). Results were expressed as arbitrary units of luminescence compared to that measured in SD group.

2.10. Cells culture and treatment

Human Hepatoma (HepG2) cells were procured from National Centre for Cell Science (NCCS, Pune, India). Cells were maintained in CO_2 incubator (Thermo scientific, forma series II 3110, USA) at 37 °C and 5% CO_2 in DMEM, supplemented with 10% FBS and 1% antibiotic antimycotic solution. Passaging of cells were done using 1X TPVG at about 80% confluency.

2.11. Treatment with palmitic acid conjugated BSA and CORM-A1

Palmitate stock solution was prepared as described previously [28]. Briefly, 100 mM PA was conjugated with 10% BSA to obtain PA (10 mM FFA/1% BSA) stock solution. PA was further diluted with media to obtain 100 μM working solution and the same was used for treatment of HepG2 cells.

2.12. Cytotoxicity assessment

HepG2 cells were seeded in 96 well plate (10^4 cells/well) in DMEM. PA (100 μM) alone or in combination with CORM-A1 (100 μM) were dosed. After 24 h 3-(4,5-dimethylthiazol-2-yl)-2,5-diphenyltetrazolium bromide (MTT; 5 mg/ml) was added and cells were incubated in the dark for 4 h. Resultant formazan crystals were dissolved in DMSO (150μL/well) and absorbance was measured at 540 nm (Synergy HTX Multimode Reader) [29].

2.13. Intracellular ROS generation by CellROX, DHE and MitoSOX staining

HepG2 cells were treated as per same treatment schedule and at the end, cells were incubated with CellROX (5 μM) for 30 min/DHE (10 μM) for 10 min/MitoSOX (5 μM) for 30 min. At the end of the incubation, the cells were washed with PBS, mounted using fluoroshield mounting medium with DAPI and photographed (Zeiss Axioplan-2 imaging fluorescence microscope).

2.14. Fluorescence activated cell-sorting (FACS) analysis

At the end of the treatment period, HepG2 cells were stained with 5 μM MitoSOX, or 50 nM MitoTracker for 30 min at 37 °C (protected from light). After washing twice, the samples were analysed using a flow cytometer (FACScalibur, BD Biosciences).

2.15. Mitochondrial membrane potential assessment by JC-1 and TMRE staining

Cells were seeded in 6 wells plate and treated as mentioned earlier. Control and treated cells were washed with 1X PBS and incubated with JC-1 (5 μg/ml) in pre-warmed 1X PBS for 30 min at 37 °C. Cells were photographed using Evos FLoid cell imaging station and fluorescent intensity was quantified using ImageJ software. TMRE (100 nM) staining was done in 1X PBS for 30 min at 37 °C. At the end of the incubation, cells were trypsinized, centrifuged at 1000g for 5 min and re-suspended in pre-warmed PBS. Fluorescence was recorded using a flow cytometer (FACScalibur, BD Biosciences).

2.16. Mitochondrial respiration (seahorse XF analyzer)

The Seahorse XFp Analyzer (Seahorse Biosciences, North Billerica, MA) was used according to the manufacturer's protocol to measure OCR and ECAR of the cells. Briefly, cells were seeded in Seahorse Flux Analyzer mini plates (10000 cells/well) and incubated overnight at 37 °C. Later, cells were treated according to the specific *in vitro* protocols, as mentioned earlier. Thereafter, the culture medium was changed to XFp base medium minimal DMEM (Seahorse Biosciences) and placed in a non-CO2 incubator at 37 °C. Mitochondrial function was assessed using the Seahorse XFp Analyzer by monitoring changes in OCR and ECAR as previously described. Three OCR measurements were obtained under basal conditions and upon sequential injection of 2 μM oligomycin, 2 μM fluoro-carbonyl-cyanide phenylhydrazone (FCCP) and 0.5 μM rotenone plus 0.5 μM antimycin A. OCR values were calculated from 3 min measurement cycles. The OCR measurements were adjusted to cell numbers. Glycolysis was assessed by analyzing ECAR in hepatocytes cultured in glucose-free medium after sequential addition of 10 mM glucose, 2 μM oligomycin and 100 mM 2-deoxyglucose. The final data were obtained using the Seahorse XFp software and calculated according their instructions.

2.17. Statistical analysis

The data were expressed as mean ± SEM and analysed by one-way analysis of variance (ANOVA), followed by Bonferroni's multiple comparison test using Graph Pad Prism 5.0 (CA, USA). *P < 0.05, **P < 0.01 and ***P < 0.001 were considered to be significant.

3. Results

3.1. CORM-A1 treatment improves NASH associated pathological changes in HFHF fed mice

CORM-A1 treatment to HFHF fed mice resulted in reduced weight gain and abdominal circumference (P < 0.0001) and showed less fat accumulation as compared to HFHF fed mice. However, no difference in food intake was observed for either of the groups (Figs. S1A–C). Results obtained in iCORM A-1 treated group were comparable to that of HFHF fed group (data not shown), thus confirming that the inactivated form was not able to elicit any response. H&E staining of visceral adipose tissue revealed larger adipocyte diameter in HFHF fed mice, but treatment with CORM-A1 significantly reduced the same and showed a mixed population of larger and medium sized adipocytes (Fig. S1D).

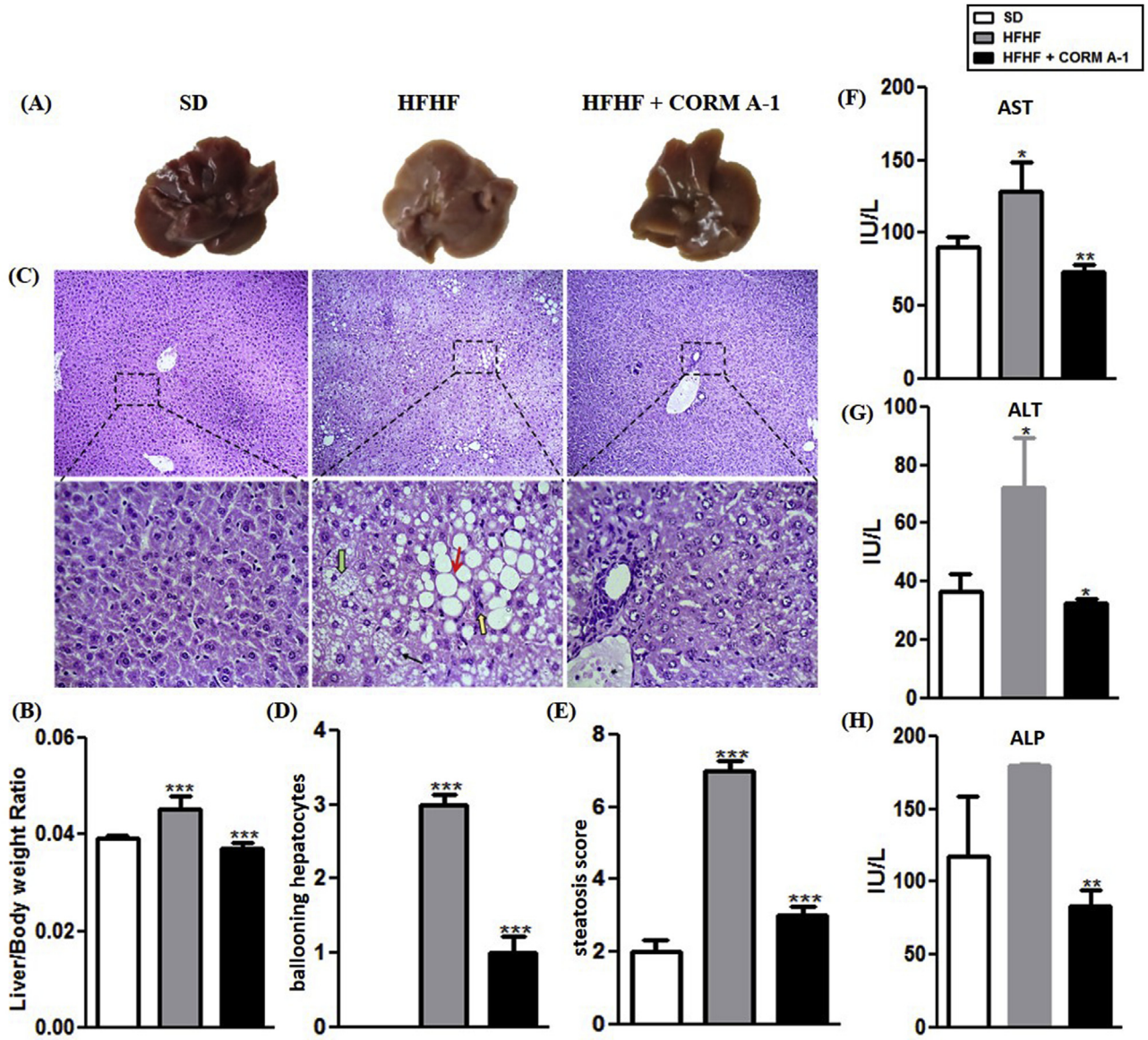

Fig. 1. Mice treated with CORM-A1 showed improvement in histopathology and functional status of liver. (A) Autopsy (B) Liver/Body weight ratio (C) H&E staining of liver section of C57BL/6J mice fed with SD, HFHF diet or HFHF + CORM-A1 (magnification 100X and 400X), **Black arrow** indicate Mallory hyaline, **Green arrow** indicate ballooning hepatocytes, **yellow arrow** indicates inflammation and **red arrow** indicate steatosis in liver (D) Scoring of ballooning hepatocytes (E) Scoring of steatosis and liver function enzymes (F) AST (G) ALT and (H) ALP. Results expressed as mean ± S.E.M. *p < 0.05, **p < 0.01 or ***p < 0.001 is when HFHF compared to SD and HFHF + CORM-A1 is compared to HFHF group. (For interpretation of the references to colour in this figure legend, the reader is referred to the Web version of this article.)

Next, we evaluated the influence of CORM-A1 on indices of metabolic profile. CORM-A1 treatment significantly improved HFHF diet-induced dysregulated serum lipid profile (Figs. S2A–H). Liver of HFHF fed mice was pale-yellow coloured and had a higher liver to body weight ratio (~35%) as compared to SD mice but the same morphometric indices in CORM-A1treated mice were comparable to SD mice (Fig. 1 A&B). Microscopic evaluation of liver tissue revealed significantly higher amount of micro vesicular hepatic steatosis, ballooning hepatocytes and mallory hyaline in HFHF fed mice. Whereas, no substantial evidence of hepatic steatosis was seen in CORM-A1 treated mice (Fig. 1C). Scoring of liver sections revealed significantly higher number of ballooning hepatocytes and increased steatosis in HFHF fed mice that was significantly decreased ($P < 0.0001$) in CORM-A1 treated group (Fig. 1 D&E). Moreover, these structural changes were associated with circulating lower levels of liver injury marker enzymes (AST, ALT and ALP) (Fig. 1F–H). Next, we investigated the impact of CORM-A1 on expression of genes associated with lipid metabolism and inflammation. CORM-A1 treatment significantly decreased the mRNA expression of key lipogenic genes (FAS and Srebp-1C) compared to HFHF fed mice. Further, mRNA expression of CD36 and CPT-1 showed non-significant changes whereas, SIRT1 showed significant upregulation in HFHF fed mice. But, CORM-A1 treatment accounted for significant increase in the mRNA levels of CD36, SIRT1 and CPT-1 in HFHF fed mice ($P < 0.01$) (Fig. S3A). Additionally, CORM-A1 treatment resulted in significant ($P < 0.009$) decrement in mRNA expression of pro-inflammatory genes, such as: interleukin 1-beta (IL-1β), interleukin-6 (IL-6) and tumor necrosis factor-alpha (TNF-α) compared to HFHF fed mice (Fig. S3B). Overall, these results show CORM-A1 improved lipid metabolism, hepatic steatosis and associated inflammation in HFHF fed mice.

3.2. CORM-A1 facilitates Nrf2 translocation, modulates Keap1 expression and activates ARE genes in liver of HFHF fed mice

Previous studies had shown that CORM-A1 exerts antioxidant

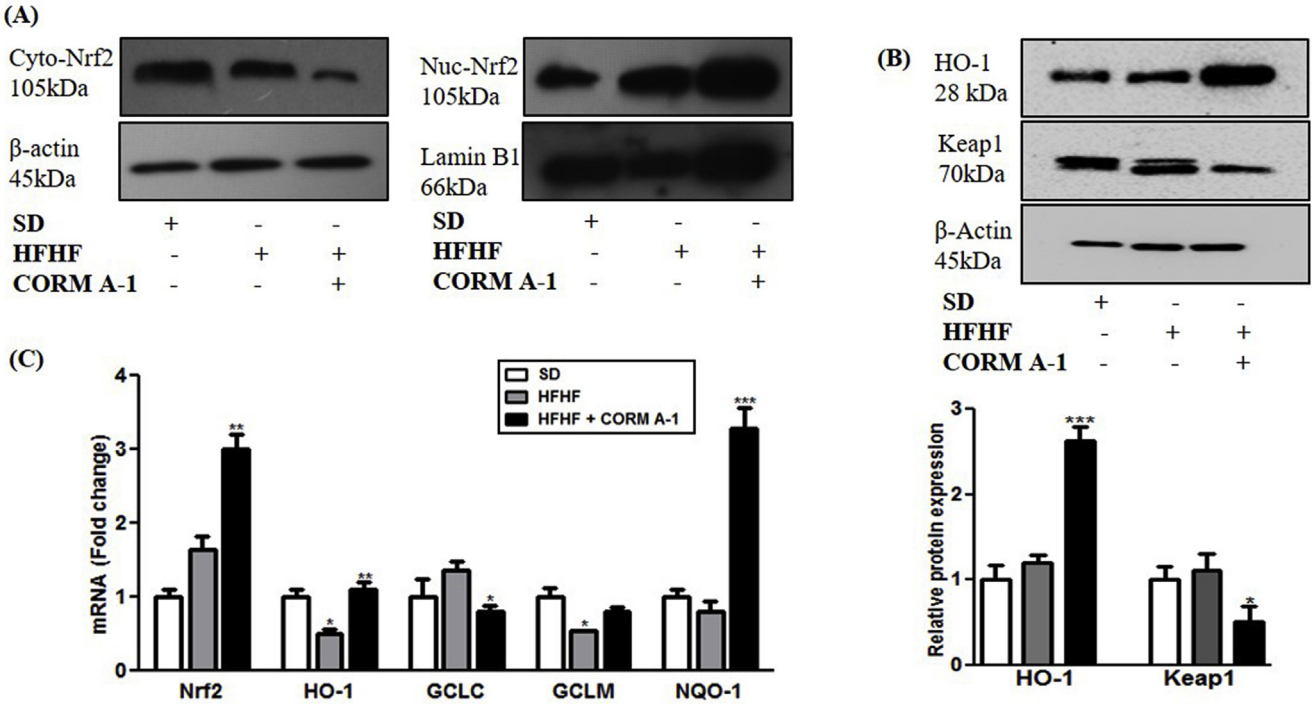

Fig. 2. CORM-A1 promotes Nrf2 translocation by modulating Keap1 expression and regulate ARE genes in liver of HFHF fed mice. C57BL/6J mice (n = 4/group) fed with SD, HFHF diet or HFHF + CORM-A1 (2 mg/kg; ip, from 9th to 16 weeks). (A) Immunoblot images of cytoplasmic and nuclear Nrf2 proteins (B) HO-1 and Keap1 proteins and their quantifications and (C) The mRNA expression of Nrf2 and related ARE genes. Results expressed as mean ± S.E.M.*p < 0.05, **p < 0.01 or ***p < 0.001 is when HFHF compared to SD and HFHF + CORM-A1 is compared to HFHF group.

activity by facilitating Nrf2 activation [25]. We evaluated Nrf2 expression in cytosolic and nuclear fraction of livers from SD, HFHF fed and HFHF + CORM-A1 treated mice. Liver of CORM-A1 treated mice showed lowered levels of Nrf2 protein in cytosol and significantly higher levels in nucleus as compared to HFHF fed mice (Fig. 2A). mRNA expression and protein content of HO-1 showed non-significant changes in HFHF fed mice, however CORM-A1 treatment significantly stimulated its expression ($P < 0.0062$). Conversely, Keap1 protein was significantly reduced in CORM-A1 treated group ($P < 0.0113$) (Fig. 2B) and this effect was associated with increased mRNA expression of ARE genes, i.e. GCLM and NQO-1 in CORM-A1 treated mice (Fig. 2C). These set of findings demonstrate that CORM-A1 promoted Nrf2 activation and subsequent upregulation of antioxidant genes in HFHF fed mice.

3.3. CORM-A1 induce changes in mRNAs associated with hepatic mitochondrial biogenesis and function in vivo

The effects of CORM-A1 on mitochondrial biogenesis and energetics was evaluated in liver of steatotic or CORM-A1 treated mice. mtDNA copy number in liver of HFHF fed mice was comparable to SD mice but, CORM-A1 treatment accounted for a significant increment ($P < 0.0001$) compared to HFHF fed mice (Fig. 3A). PGC-1α and NRF-1 mRNA expression directly regulate the mitochondrial number as well as other metabolic events in steatotic mice [30]. We also observed a significant increment in mRNA expression and protein content of PGC-1α and NRF-1 in HFHF fed mice, which were further significantly elevated in CORM-A1 treated mice as compared to HFHF fed mice. mRNA levels of regulators of mitochondrial fission (Drp1) and mtDNA (TFAM) was unchanged and elevated in the liver of HFHF fed and CORM-A1 treated mice respectively (Fig. 3B&C). Additionally, the functional status of mitochondria was studied by assessing hepatic ATP production. Data showed that ATP content in liver of HFHF fed mice was significantly lower than SD mice. CORM-A1 treatment was instrumental in increasing the ATP production significantly ($P < 0.002$) to match the levels measured in SD mice (Fig. 3D). These findings indicate that HFHF fed mice showed unaltered mitochondrial number but compromised ATP production and this was significantly improved with CORM-A1 treatment.

3.4. CORM-A1 improves oxidative stress and cell survival via Nrf2 translocation and activation of ARE genes in hepatocytes

Our findings are suggesting that the anti-NASH potential of CORM-A1 in HFHF fed mice involves the activation of Nrf2-ARE pathway. Progression of hepatic steatosis comprises of multiple overlapping molecular events. Hence, we carried out molecular studies using human hepatocellular cell line (HepG2) to confirm and explain our *in vivo* findings. PA-treatment to hepatic cells mimics the condition of second hit of NALFD progression via higher ROS generation and cell death [31]. PA treated HepG2 cells resulted in ~50% reduction in cell viability but CORM-A1 (100 μm) treated group recorded relatively more (~68%) viable cells. PA treatment resulted in heightened levels of intracellular ROS as evidenced by DHE (red) and CellROX (green) staining but CORM-A1 co-supplementation resulted in significant decrement in red and green fluorescence respectively (Fig. 4A&B), thus suggesting decreased ROS production. Translocation of Nrf2 protein from cytoplasm to nucleus was further confirmed in HepG2 cells wherein, CORM-A1 treatment accounted for significantly higher nuclear accumulation of Nrf2 as compared to PA treated cells (Fig. 4C). Western blot analysis of Keap1 protein (negative regulator of Nrf2) showed a significant decrement in PA and CORM-A1 treated groups. Additionally, co-immunoprecipitation (co-IP) studies results revealed a time-depended decrement in Keap1/Nrf2 interaction after treatment with CORM-A1 to HepG2 cells (Fig. 4D). Further, an increase in HO-1 mRNA and protein were recorded in PA treated cells whereas, more pronounced effect in mRNA and an increment in protein was noted in CORM-A1 co-supplemented group. Other ARE genes viz. GCLC, GCLM and NQO-1 were also studied wherein, GCLM mRNA levels was

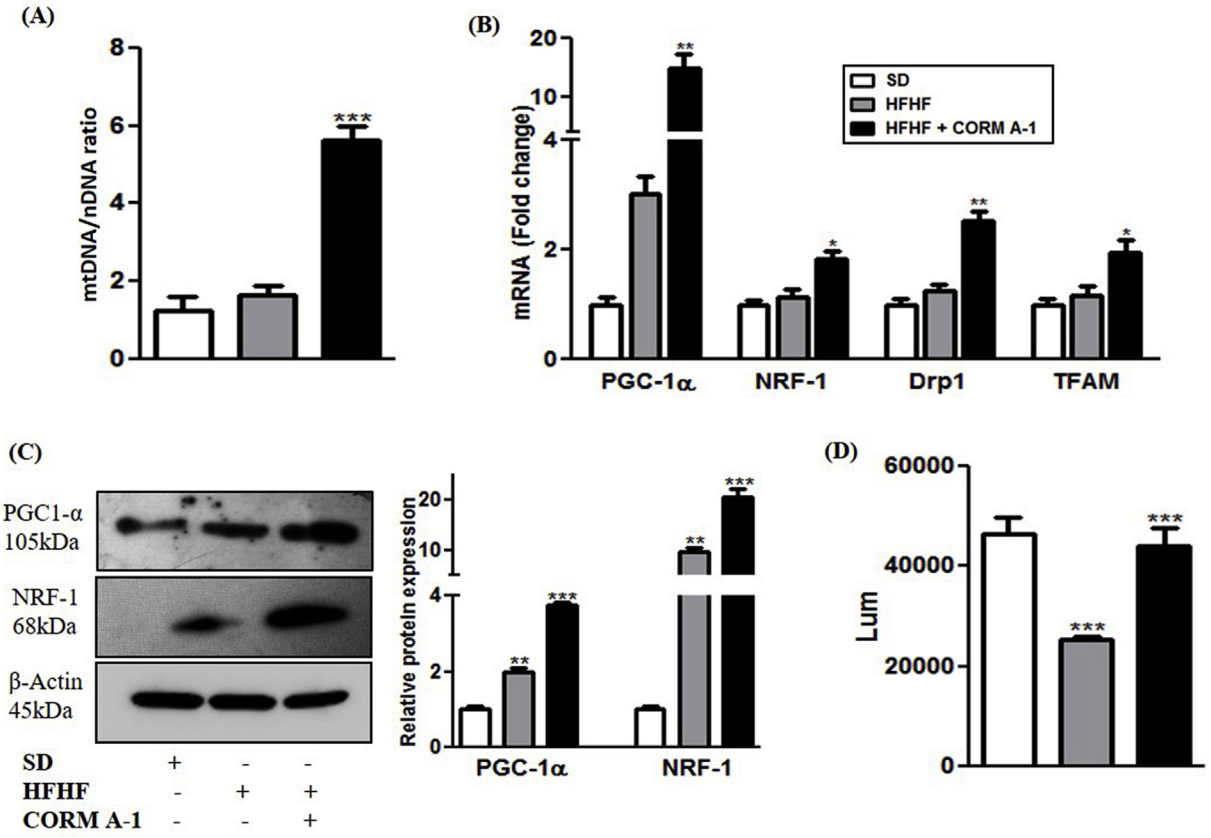

Fig. 3. CORM-A1 treatment improves hepatic mitochondrial biogenesis and function. C57BL/6J mice (n = 4/group) fed with SD, HFHF diet or HFHF + CORM-A1 (2 mg/kg; ip, from 9th to 16 weeks). (A) mtDNA content (B) Hepatic mRNA expression of genes related to mitochondrial biogenesis (C) Immunoblot images of regulatory proteins of mitochondrial biogenesis and their quantifications and (D) cellular ATP levels. Results expressed as mean ± S.E.M. *p < 0.05, **p < 0.01 or ***p < 0.001 is when HFHF compared to SD and HFHF + CORM-A1 is compared to HFHF group.

decreased significantly following PA treatment. But, GCLC and NQO-1 mRNA levels in the same group showed non-significant changes. CORM-A1 co-supplementation to PA treated HepG2 cells was marked by significantly elevated mRNA levels of GCLC, GCLM and NQO-1 (Fig. 4E&F).

3.5. PA-mediated impaired mitochondrial oxidative stress, membrane potential and mass in HepG2 cells is alleviated by the antioxidant potential of CORM-A1

PA-treated HepG2 cells are a known model to study mitochondrial dysfunction [32]. Mitochondrial specific ROS was accessed by MitoSOX staining of HepG2 cells. Imaging and FACS analysis revealed prominent red fluorescence (higher ROS) in PA treated HepG2 cells whereas a weaker fluorescence (lower ROS) was recorded in CORM-A1 co-supplemented group (Fig. 5A-i&ii). JC-1 staining forms red coloured J-aggregates whereas, a decrease in red/green fluorescence intensity ratio marks mitochondrial depolarization. We recorded a shift in fluorescence intensity ratio (towards green) in PA treated HepG2 cells as compared to the control. CORM-A1 co-supplementation for 12 h accounted for higher indices of fluorescence (red/green ratio) suggesting improved mitochondrial membrane potential (MMP) (Fig. 5B-i&ii). Likewise, FACS analysis using TMRE stain was performed to assess ΔΨm wherein, PA-treated HepG2 cells recorded a significant decrement ($P < 0.0001$) compared to control cells. CORM-A1 co-treatment improved ΔΨm as evidenced by significant increment in fluorescence intensity of HepG2 cells (Fig. 5C). Mitotracker dye stains mitochondria irrespective of MMP and hence, the fluorescence intensity is indicative of the total mitochondrial mass. Weak fluorescence ($P < 0.0001$) recorded in PA-treated HepG2 cells in contrast was prominent in CORM-A1 treated cells (Fig. 6A-i&ii).

3.6. CORM-A1 improves PA-abrogated mitochondrial biogenesis and respiration in HepG2 cells

Mitochondrial biogenesis regulatory mRNAs and protein contents in HepG2 cells were also assessed in response to the different treatments. PA significantly reduced mRNA levels of PGC-1α and NRF-1, however CORM-A1 co-supplementation rescued their expression (Fig. 6B). Protein levels of PGC-1α was decreased and NRF-1 was increased in PA treated HepG2 cells. CORM A1 treatment accounted for a significant increase ($P < 0.01$) in protein levels of PGC-1α and NRF-1 (Fig. 6C). mRNA levels of other key genes controlling mitochondrial fission and mtDNA copy number, such as Drp1 and TFAM were significantly downregulated in PA-treated HepG2 cells. Though, CORM-A1 did not induce major changes in mRNA expression of TFAM but a significant increment was observed in Drp1 ($P < 0.001$). Furthermore, in PA treated HepG2 cells we observed a significant decrement in mtDNA content that was significantly improved ($P < 0.05$) by CORM-A1 treatment (Fig. 6D). These findings are in agreement with our results obtained *in vivo*. As mitochondrial oxidative stress and redox imbalance are implicated in progression to NASH [33], we further assessed mitochondrial function by seahorse XF extracellular flux analyzer, as measures of oxygen consumption rate (OCR) and glycolytic activity assessing lactic acid production and extracellular release (ECAR). CORM-A1 accounted for higher basal respiration rate than PA treated cells or control group. In the next step, addition of oligomycin resulted in respiration linked to ATP production and proton leak. A significant

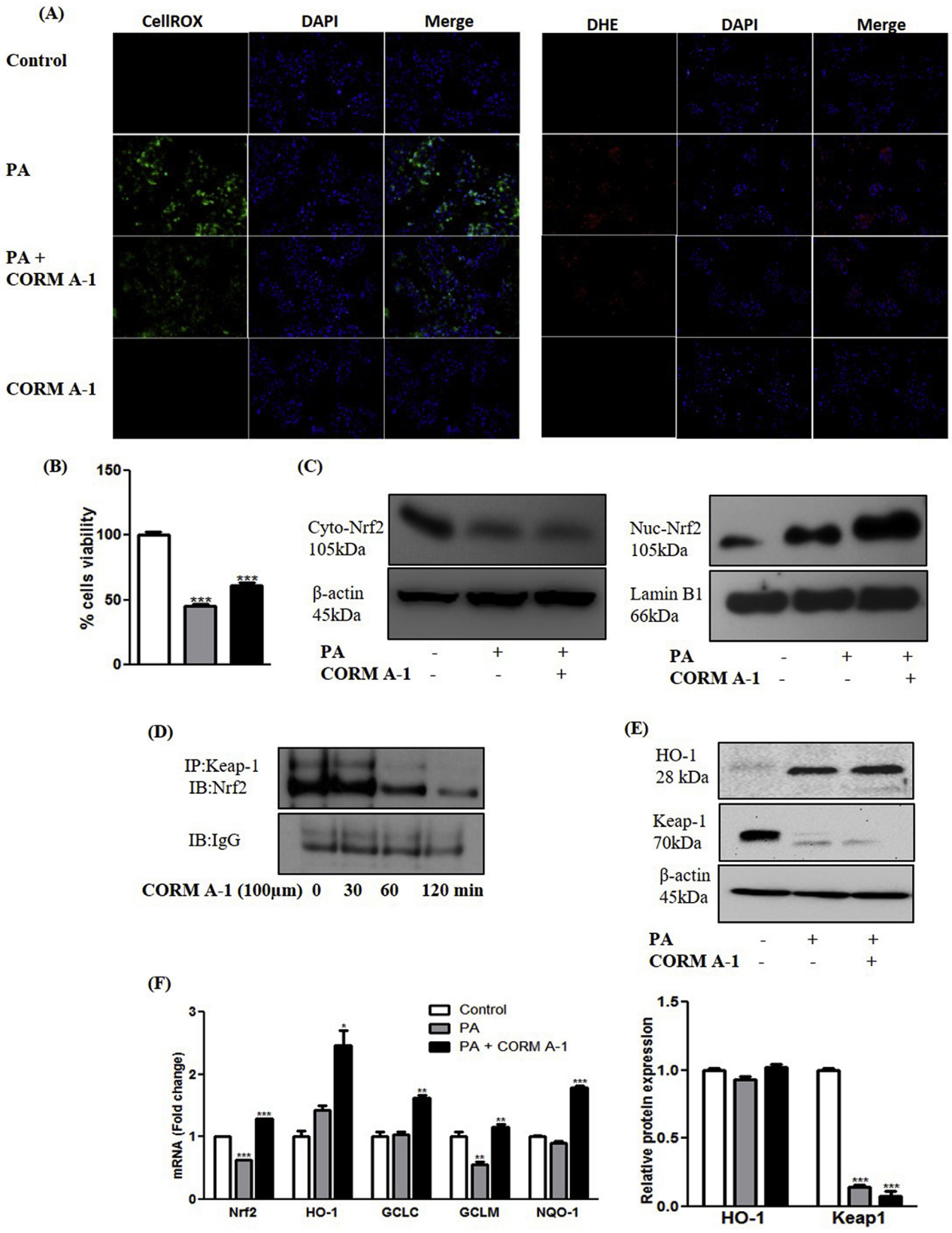

Fig. 4. CORM-A1 improves oxidative stress and cell survival via Nrf2 translocation and activation of ARE genes in hepatocytes. HepG2 cells were treated with PA (100 μm) in presence and absence of CORM-A1 (100 μm). Oxidative stress in HepG2 cells was evaluated using (A) CellROX and DHE stain in control, PA, PA + CORM-A1 and CORM-A1 groups. Cell survival was determine using (B) cell viability assay (MTT) (C) Nrf2 translocation was checked using immunoblot analysis in cytoplasm and nucleus (D) co-immunoprecipitation demonstrating time depended decrement in keap1 protein (E) qualitative and quantitative levels of HO-1 and Keap1 proteins and (F) expression levels of antioxidant gene was recorded using qPCR analysis. Results expressed as mean ± S.E.M. *$p < 0.05$, **$p < 0.01$ or ***$p < 0.001$ is when PA treatment is compared to control cells and PA + CORM-A1 is compared to PA alone group.

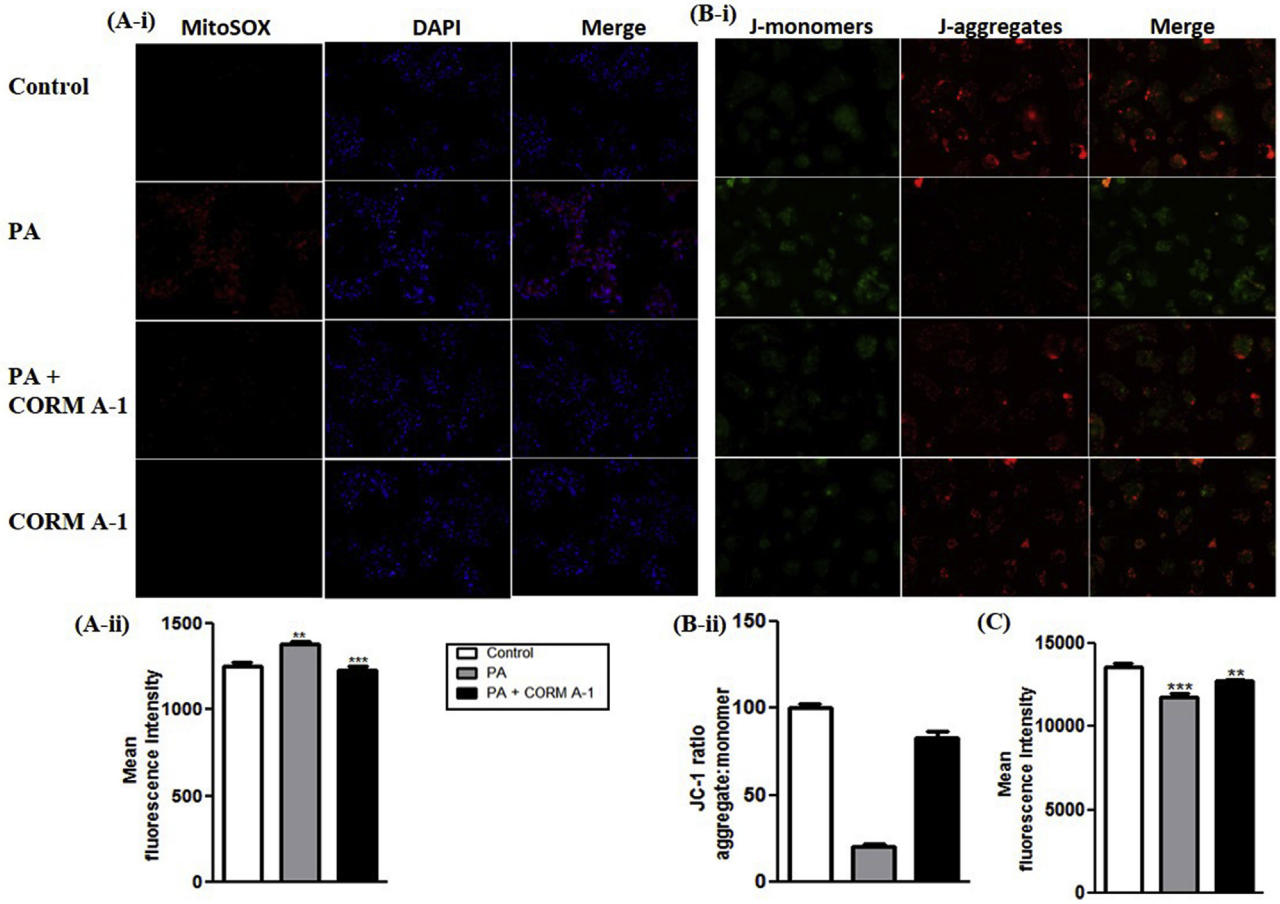

Fig. 5. CORM-A1 improves mitochondrial oxidative stress and membrane potential in PA treated HepG2 cells. Mitochondria specific ROS and MMP was measured in HepG2 cells treated with PA (100 μm) in presence and absence of CORM-A1 (100 μm) for 12 h. Cells stained with (A i&ii) MitoSOX and their fluorescence intensity (B i&ii) JC-1 staining for measuring MMP and its fluorescence intensities measured using FACS analysis and (C) fluorescence intensities of TMRE stain. Results expressed as mean ± S.E.M. *p < 0.05, **p < 0.01 or ***p < 0.001 is when PA treatment is compared to control cells and PA + CORM-A1 is compared to PA alone group.

decrement in ATP production was also observed by PA treatment but CORM-A1 accounted for a significant increment ($P < 0.001$). Further, PA treatment showed diminished proton leak, but CORM-A1 treated cells showed a significant increment ($P < 0.001$). Addition of FCCP is known to maximize mitochondrial respiratory capacity whereas; rotenone blocks complex I and inhibits oxidative phosphorylation [34]. The same also enables the detection of spare respiratory capacity. In our study, PA treatment resulted in significant decrement in indices of maximal cellular respiration and spare respiratory capacity, but CORM-A1 treatment significantly improved these parameters in PA treated HepG2 cells (Fig. 7A&B).

The extracellular acidification rate is indicative of glycolytic activity in absence of mitochondrial respiration. Maximum ECAR or glycolytic capacity observed in PA treated cells was significantly diminished, in agreement with indices of glycolysis and glycolytic reserve. CORM-A1 treatment improved the glycolytic capacity and glycolytic reserve, however maximum ECAR values showed a non-significant increment. Indices of non-glycolytic acidification in PA-treated cells with or without CORM-A1 showed a non-significant increment (Fig. 7C&D). These results suggest that co-supplementation of CORM-A1 increases mitochondrial oxidative phosphorylation in PA treated HepG2 cells.

4. Discussion

We have investigated the protective effects of the antioxidant gasotransmitter CORM-A1 in a mouse model of NASH. Owing to the multifactorial nature of NASH and resultant morbidity and mortality [35], an effective therapeutic strategy should involve a multipronged approach with a synergistic effect on various facets of liver function. Herein, we show that treatments of HFHF mice, an established model of NASH, with CORM-A1 resulted in significant hepatoprotection at multiple levels.

In our study, HFHF diet was fed to C57BL/6J mice to mimic fructose and fat rich foods that are known to be associated with life style disorders [36]. In these mice, we observed significant elevation in titers of circulating liver injury markers along with fatty manifestations in liver histology thus, providing evidence on steatotic changes. In addition, steatotic mice showed elevated serum lipid profile, ballooned hepatocytes, impaired redox and lipid homeostasis and lowered ATP production. These observations are in agreement with other reports on HFHF diet-induced NASH where fructose feeding is known to deplete ATP production and suppress mitochondrial fatty acid oxidation resulting in increased production of ROS [37]. Remarkably, CORM-A1 treatment to HFHF fed mice showed a significant improvement in the said histopathological and biochemical/functional parameters.

In acetaminophen-treated mice, we have previously reported that, the hepatoprotective effects of CORM-A1 involve its ability to promote antioxidant responses through the activation of Nrf2 [25]. Experimental and clinical studies have reported a strong association between severity of NASH and degree of oxidative stress [38]. Herein, CORM-A1-mediated induction of Nrf2-ARE pathway provides protection against oxidative stress induced by PA/HFHF diet. Augmented nuclear

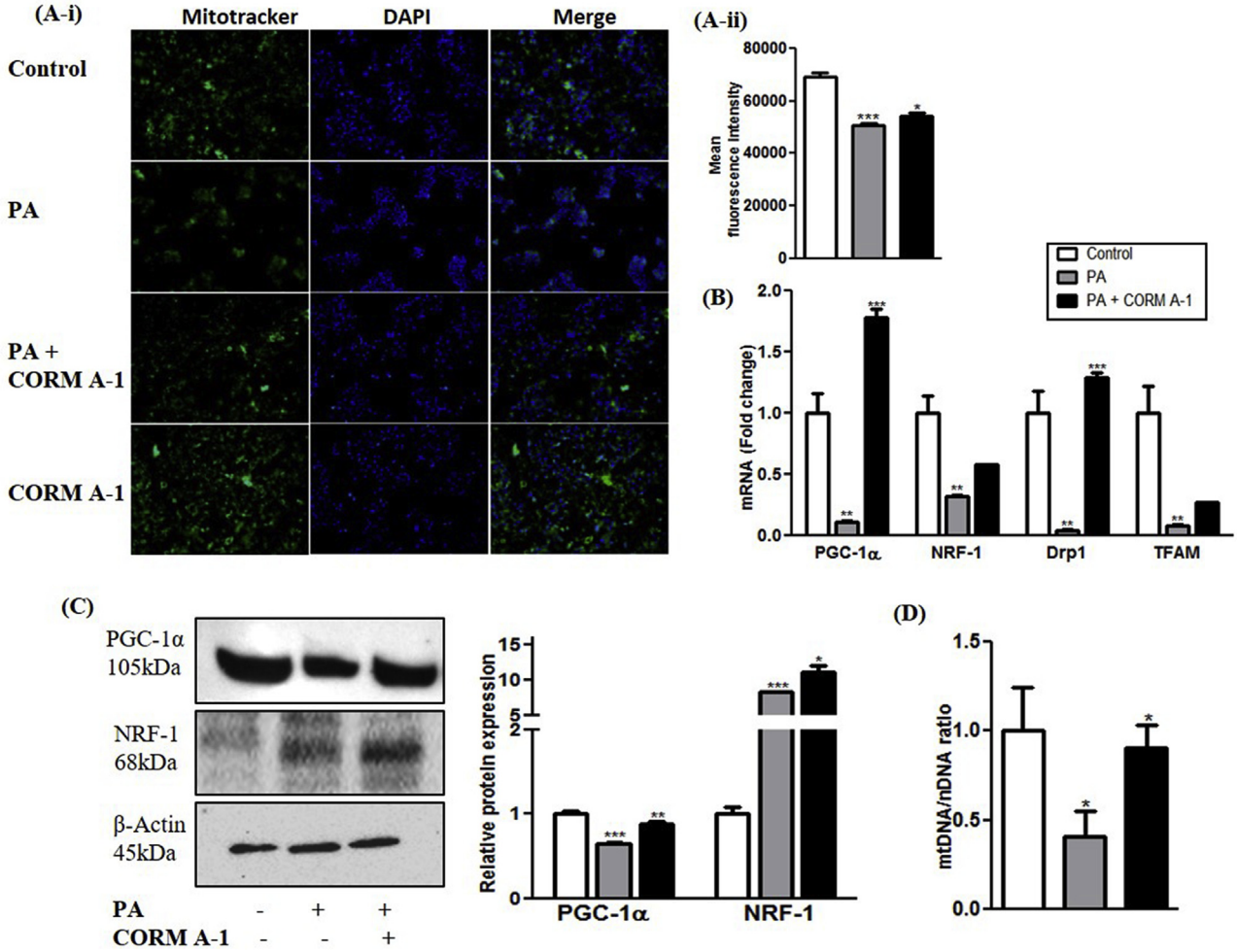

Fig. 6. CORM-A1 improves mitochondrial mass and biogenesis in PA treated HepG2 cells. Cells were treated for 24 h with PA and PA + CORM-A1 wherein, (A i &ii) Mitotracker staining and its fluorescence intensity (B) mRNA expression of regulatory genes for mitochondrial biogenesis (C) immunoblot images and their quantification and (D) mtDNA content. Results expressed as mean ± S.E.M. *p < 0.05, **p < 0.01 or ***p < 0.001 is when PA treatment is compared to control cells and PA + CORM-A1 is compared to PA alone group.

translocation/activation of Nrf2 was observed in *in vivo* and *in vitro* CORM-A1treated groups and was confirmed by consequent up-regulation of ARE genes such as: HO-1, GCLC, GCLM and NQO-1. Further, CORM-A1-mediated Nrf2 nuclear translocation was seen in HepG2 cells with time-dependent dissociation from its negative regulator Keap1, thus, confirming our previous study using *in silico* docking analysis of CO and showing that CORM-A1 promotes Nrf2 activation via CO-mediated release of Nrf2 from Keap1 [25].

Oxidation of fatty acids is a high energy yielding process along with production of excessive ROS that is kept under control by the cellular antioxidant defense system. However, systemic and intracellular lipid overload, ROS and redox imbalance leads to GSH depletion, apoptosis and cell death [39]. Additionally, previous studies had reported that various Nrf2 activators can improve lipid metabolism [40]. In our study we observed significant decrease in fatty acid synthesis and enhanced clearance/catabolism of lipids from the steatotic liver following CORM-A1 treatment.

Apart from its role as a transcriptional activator of cellular antioxidants, Nrf2 is also involved in maintaining mitochondrial homeostasis [41]. In NASH, mitochondrial dysfunction plays a crucial role because of its involvement in β-oxidation of fatty acids and the same has also been implicated in first and second hits of NASH [42]. Hence, we evaluated the influence of CORM-A1-induced Nrf2 signaling on mitochondrial functions in PA treated HepG2 cells. PA has been preferred over stearic and oleic acids for its ability to induced mitochondrial dysfunction in HepG2 cells [32]. CORM-A1 co-supplemented HepG2 cells showed reduced intracellular and mitochondria ROS formation along with a significant improvement in MMP. Since MMP has been implicated as an indicator of cellular metabolic status, the reduced ROS (DHE and CellROX) and improved MMP (JC-1 and TMRE) can be attributed to Nrf2-mediated control of cellular redox homeostasis [42].

Additionally, CORM-A1 increased mtDNA copy number in PA-treated HepG2 cells or in liver of HFHF fed mice, a mechanism also attributable to Nrf2 activation and resulting in mitochondrial biogenesis, as suggested by the reported effects of Nrf2-dependent translational activation of NRF-1 [43] and by the elevation of the transcriptional co-activator PGC-1α [30]. The specific contribution of Nrf2 in maintaining NRF-1 and PGC-1α expressions was reported in liver of Nrf2 knockout mice [41]. Our data also showed that CORM-A1 treatment accounted for significantly higher levels of TFAM and Drp1 mRNAs. TFAM is a mitochondria specific transcription factor involved in replication of mitochondrial genome and in maintenance of mtDNA copy number [44], whereas Drp1 regulates mitochondrial fission and is a potential therapeutic target in metabolic diseases [45].

PA has been reported to cause ROS production and hyperpolarization of mitochondria. This scenario is mitigated at cellular level by increasing proton leak [46,47]. Also, PA causes accumulation of

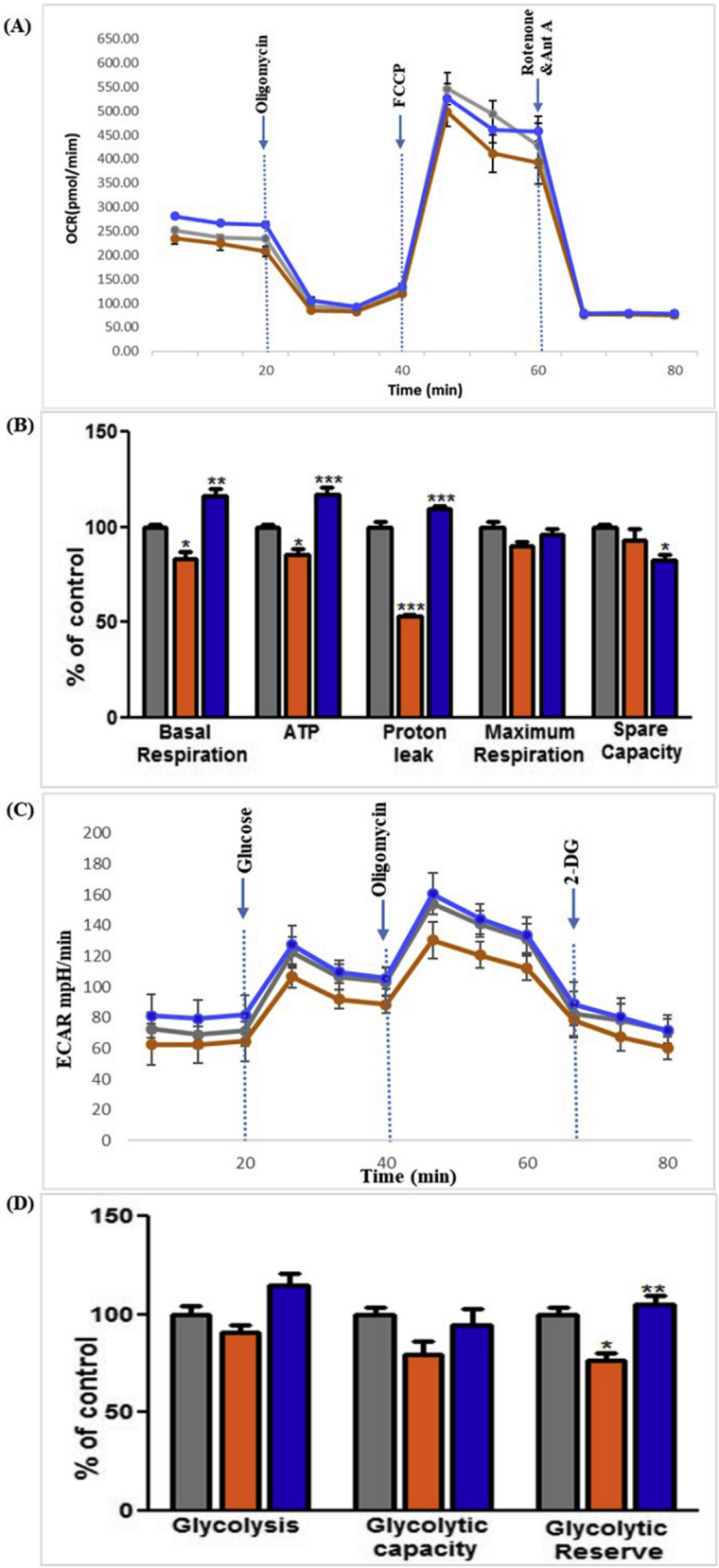

Fig. 7. CORM-A1 improves PA-abrogated respiration in HepG2 cells. HepG2 cells were treated with PA (100 μm) in presence and absence of CORM-A1 (100 μm) for 24 h. Cell respiration were measured as Oxygen consumption rate (OCR) and extracellular acidification rate (ECAR) and quantification was done using Seahorse XFe 96 Metabolic Flux Analyzer. (A) mitochondrial respiration measured as OCR (B) quantification of other respiratory parameters (Basal respiration, ATP, Proton leak, maximum respiration and spare capacity) using OCR data. (C) glycolytic lactic acid production (non-mitochondrial respiration) measured as ECAR (D) calculated values for glycolysis, glycolytic capacity and reserves from ECAR data. Results expressed as mean ± S.E.M. *p < 0.05, **p < 0.01 or ***p < 0.001 is when PA treatment is compared to control cells and PA + CORM-A1 is compared to PA alone group.

pyruvate leading to a decrease in basal and maximal mitochondrial respiratory rate that shifts the OCR to ECAR by increasing glycolytic flux [48]. Our findings of improved basal respiration in PA + CORM-A1 treated HepG2 cells, accompanied by a significant increment in proton leak is the cause for observed higher ATP production. CO induced increase in proton leak is the reported cause for a higher uncoupling activity in isolated mitochondria and in experimentally induced insulin resistance in obese mice [49–51]. PA depressed ATP levels and

abrogated mitochondrial respiration due to a compensatory higher metabolic flux in hepatocytes that led to poor cell viability. An increment in non-mitochondrial ATP generation through glycolysis in early phase has been reported. In advanced stages of hepatic steatosis the ATP reserves are depleted [52]. However, CORM-A1 co-supplementation to PA treated HepG2 cells accounted for higher indices of glycolytic reserves thus implying towards a healthy state of mitochondria and less dependency on non-mitochondrial respiration.

In summary, the results of our study evidencing CORM-A1-mediated amelioration of mitochondrial function in steatotic liver via Nrf2, is the first to directly suggest the therapeutic potential of CORM-A1 for the clinical management of NASH and fatty liver.

Declaration of interests

The authors declare no competing interests.

Acknowledgment

The author KKU is thankful to University Grant Commission for providing financial assistance in form of RFSMS fellowship F.25-1/2013-14(BSR)5-71/2007(BSR) Dt. 30/05/2014 and DST-SERB (ITS/2018/004528) for providing travel support during my visit to USA. Help rendered by Dr. Bartoli's Lab staff is duly acknowledged. Authors are also thankful to Prof. Rajesh Singh, Department of Biochemistry, MSU Baroda for extending real time thermal cycler facility and Dr. Kishore Rajput, Department of Botany, MSU Baroda for microscopy.

Appendix A. Supplementary data

Supplementary data to this article can be found online at https://doi.org/10.1016/j.redox.2019.101314.

References

[1] Y. Cheng, K. Zhang, Y. Chen, Y. Li, Y. Li, K. Fu, R. Feng, Associations between dietary nutrient intakes and hepatic lipid contents in NAFLD patients quantified by 1H-MRS and dual-Echo MRI, Nutrients 8 (9) (2016) 527.
[2] C.P. Day, Genetic and environmental susceptibility to non-alcoholic fatty liver disease, Dig. Dis. 28 (1) (2010) 255–260.
[3] Z. Younossi, Q.M. Anstee, M. Marietti, T. Hardy, L. Henry, M. Eslam, J. George, E. Bugianesi, Global burden of NAFLD and NASH: trends, predictions, risk factors and prevention, Nat. Rev. Gastroenterol. Hepatol. 15 (1) (2018) 11.
[4] M. Fuchs, A.J. Sanyal, Lipotoxicity in NASH, J. Hepatol. 56 (1) (2012) 291–293.
[5] A.M. Oseini, A.J. Sanyal, Therapies in non-alcoholic steatohepatitis (NASH), Liver Int. 37 (2017) 97–103.
[6] D. Pessayre, B. Fromenty, NASH: a mitochondrial disease, J. Hepatol. 42 (6) (2005) 928–940.
[7] K. Begriche, A. Igoudjil, D. Pessayre, B. Fromenty, Mitochondrial dysfunction in NASH: causes, consequences and possible means to prevent it, Mitochondrion 6 (1) (2006) 1–28.
[8] A.M. Diehl, Cytokine regulation of liver injury and repair, Immunol. Rev. 174 (1) (2000) 160–171.
[9] S.S. Chambel, A. Santos-Gonçalves, T.L. Duarte, The dual role of Nrf2 in nonalcoholic fatty liver disease: regulation of antioxidant defenses and hepatic lipid metabolism, BioMed Res. Int. 2015 (2015).
[10] J.B. de Haan, Nrf2 activators as attractive therapeutics for diabetic nephropathy, Diabetes 60 (11) (2011) 2683–2684.
[11] R.N. Jadeja, K.K. Upadhyay, R.V. Devkar, S. Khurana, Naturally occurring Nrf2 activators: potential in treatment of liver injury, Oxid. Med. Cell. Longev. 2016 (2016).
[12] W. Liu, D. Wang, K. Liu, X. Sun, Nrf2 as a converging node for cellular signaling pathways of gasotransmitters, Med. Hypotheses 79 (3) (2012) 308–310.
[13] R. Tenhunen, H.S. Marver, R. Schmid, The enzymatic conversion of heme to bilirubin by microsomal heme oxygenase, Proc. Natl. Acad. Sci. 61 (2) (1968) 748–755.
[14] J. Boczkowski, J.J. Poderoso, R. Motterlini, CO–metal interaction: vital signaling from a lethal gas, Trends Biochem. Sci. 31 (11) (2006) 614–621.
[15] E.O. Owens, Endogenous carbon monoxide production in disease, Clin. Biochem. 43 (15) (2010) 1183–1188.
[16] S.W. Ryter, A.M. Choi, Carbon monoxide in exhaled breath testing and therapeutics, J. Breath Res. 7 (1) (2013) 017111.
[17] R. Motterlini, L.E. Otterbein, The therapeutic potential of carbon monoxide, Nat. Rev. Drug Discov. 9 (9) (2010) 728.
[18] K. Taguchi, S. Nagao, H. Maeda, H. Yanagisawa, H. Sakai, K. Yamasaki, T. Wakayama, H. Watanabe, M. Otagiri, T. Maruyama, Biomimetic carbon monoxide delivery based on hemoglobin vesicles ameliorates acute pancreatitis in mice via the regulation of macrophage and neutrophil activity, Drug Deliv. 25 (1) (2018) 1266–1274.
[19] P. Cabrales, A.G. Tsai, M. Intaglietta, Hemorrhagic shock resuscitation with carbon monoxide saturated blood, Resuscitation 72 (2) (2007) 306–318.
[20] R. Motterlini, B.E. Mann, R. Foresti, Therapeutic applications of carbon monoxide-releasing molecules, Expert Opin. Investig. Drugs 14 (11) (2005) 1305–1318.
[21] R. Motterlini, P. Sawle, J. Hammad, S. Bains, R. Alberto, R. Foresti, C.J. Green, CORM-A1: a new pharmacologically active carbon monoxide-releasing molecule, FASEB J. 19 (2) (2005) 284–286.
[22] I. Nikolic, T. Saksida, M. Vujicic, I. Stojanovic, S. Stosic-Grujicic, Anti-diabetic actions of carbon monoxide-releasing molecule (CORM)-A1: immunomodulation and regeneration of islet beta cells, Immunol. Lett. 165 (1) (2015) 39–46.
[23] J. Varadi, I. Lekli, B. Juhasz, I. Bacskay, G. Szabo, R. Gesztelyi, L. Szendrei, E. Varga, I. Bak, R. Foresti, Beneficial effects of carbon monoxide-releasing molecules on post-ischemic myocardial recovery, Life Sci. 80 (17) (2007) 1619–1626.
[24] P. Fagone, K. Mangano, S. Mammana, E. Cavalli, R. Di Marco, M.L. Barcellona, L. Salvatorelli, G. Magro, F. Nicoletti, Carbon monoxide-releasing molecule-A1 (CORM-A1) improves clinical signs of experimental autoimmune uveoretinitis (EAU) in rats, Clin. Immunol. 157 (2) (2015) 198–204.
[25] K.K. Upadhyay, R.N. Jadeja, J.M. Thadani, A. Joshi, A. Vohra, V. Mevada, R. Patel, S. Khurana, R.V. Devkar, Carbon monoxide releasing molecule A-1 attenuates acetaminophen-mediated hepatotoxicity and improves survival of mice by induction of Nrf2 and related genes, Toxicol. Appl. Pharmacol. 360 (2018) 99–108.
[26] S. Love, M.A. Mudasir, S.C. Bhardwaj, G. Singh, S.A. Tasduq, Long-term administration of tacrolimus and everolimus prevents high cholesterol-high fructose-induced steatosis in C57BL/6J mice by inhibiting de-novo lipogenesis, Oncotarget 8 (69) (2017) 113403.
[27] W. Liang, A.L. Menke, A. Driessen, G.H. Koek, J.H. Lindeman, R. Stoop, L.M. Havekes, R. Kleemann, A.M. van den Hoek, Establishment of a general NAFLD scoring system for rodent models and comparison to human liver pathology, PLoS One 9 (12) (2014) e115922.
[28] S.P. Cousin, S.R. Hügl, C.E. Wrede, H. Kajio, M.G. Myers Jr., C.J. Rhodes, Free fatty acid-induced inhibition of glucose and insulin-like growth factor I-induced deoxyribonucleic acid synthesis in the pancreatic β-cell line INS-1, Endocrinology 142 (1) (2001) 229–240.
[29] S. Jana, D. Patel, S. Patel, K. Upadhyay, J. Thadani, R. Mandal, S. Das, R. Devkar, Anthocyanin rich extract of Brassica oleracea L. alleviates experimentally induced myocardial infarction, PLoS One 12 (8) (2017) e0182137.
[30] R.C. Scarpulla, Metabolic control of mitochondrial biogenesis through the PGC-1 family regulatory network, Biochim. Biophys. Acta Mol. Cell Res. 1813 (7) (2011) 1269–1278.
[31] M. Ricchi, M.R. Odoardi, L. Carulli, C. Anzivino, S. Ballestri, A. Pinetti, L.I. Fantoni, F. Marra, M. Bertolotti, S. Banni, Differential effect of oleic and palmitic acid on lipid accumulation and apoptosis in cultured hepatocytes, J. Gastroenterol. Hepatol. 24 (5) (2009) 830–840.
[32] I. García-Ruiz, P. Solís-Muñoz, D. Fernández-Moreira, T. Muñoz-Yagüe, J.A. Solís-Herruzo, In vitro treatment of HepG2 cells with saturated fatty acids reproduces mitochondrial dysfunction found in nonalcoholic steatohepatitis, Dis. Model. Mech. 8 (2) (2015) 183–191.
[33] M. Pérez-Carreras, P. Del Hoyo, M.A. Martın, J.C. Rubio, A. Martın, G. Castellano, F. Colina, J. Arenas, J.A. Solis-Herruzo, Defective hepatic mitochondrial respiratory chain in patients with nonalcoholic steatohepatitis, Hepatology 38 (4) (2003) 999–1007.
[34] A. Iuso, B. Repp, C. Biagosch, C. Terrile, H. Prokisch, Assessing Mitochondrial Bioenergetics in Isolated Mitochondria from Various Mouse Tissues Using Seahorse XF96 Analyzer, Mitochondria, Springer, 2017, pp. 217–230.
[35] C. Estes, H. Razavi, R. Loomba, Z. Younossi, A.J. Sanyal, Modeling the epidemic of nonalcoholic fatty liver disease demonstrates an exponential increase in burden of disease, Hepatology 67 (1) (2018) 123–133.
[36] J.E. Mells, P.P. Fu, S. Sharma, D. Olson, L. Cheng, J.A. Handy, N.K. Saxena, D. Sorescu, F.A. Anania, Glp-1 analog, liraglutide, ameliorates hepatic steatosis and cardiac hypertrophy in C57BL/6J mice fed a Western diet, Am. J. Physiol. Gastrointest. Liver Physiol. 302 (2) (2011) G225–G235.
[37] M.A. Lanaspa, L.G. Sanchez-Lozada, Y.-J. Choi, C. Cicerchi, M. Kanbay, C.A. Roncal-Jimenez, T. Ishimoto, N. Li, G. Marek, M. Duranay, Uric Acid induces hepatic steatosis by generation of mitochondrial oxidative stress potential role in fructose-dependent and-independent fatty liver, J. Biol. Chem. 287 (48) (2012) 40732–40744.
[38] Y. Sumida, E. Niki, Y. Naito, T. Yoshikawa, Involvement of free radicals and oxidative stress in NAFLD/NASH, Free Radic. Res. 47 (11) (2013) 869–880.
[39] V. Ribas, C. García-Ruiz, J.C. Fernández-Checa, Glutathione and mitochondria, Front. Pharmacol. 5 (2014) 151.
[40] N.R. Kitteringham, A. Abdullah, J. Walsh, L. Randle, R.E. Jenkins, R. Sison, C.E. Goldring, H. Powell, C. Sanderson, S. Williams, Proteomic analysis of Nrf2 deficient transgenic mice reveals cellular defence and lipid metabolism as primary Nrf2-dependent pathways in the liver, J. Proteomics 73 (8) (2010) 1612–1631.
[41] A.T. Dinkova-Kostova, A.Y. Abramov, The emerging role of Nrf2 in mitochondrial function, Free Radic. Biol. Med. 88 (2015) 179–188.
[42] S. Kovac, P.R. Angelova, K.M. Holmström, Y. Zhang, A.T. Dinkova-Kostova, A.Y. Abramov, Nrf2 regulates ROS production by mitochondria and NADPH oxidase, Biochim. Biophys. Acta Gen. Subj. 1850 (4) (2015) 794–801.
[43] C.A. Piantadosi, M.S. Carraway, A. Babiker, H.B. Suliman, Heme oxygenase-1 regulates cardiac mitochondrial biogenesis via Nrf2-mediated transcriptional control of nuclear respiratory factor-1, Circ. Res. 103 (11) (2008) 1232–1240.
[44] J.L. Pohjoismäki, S. Wanrooij, A.K. Hyvärinen, S. Goffart, I.J. Holt, J.N. Spelbrink,

H.T. Jacobs, Alterations to the expression level of mitochondrial transcription factor A, TFAM, modify the mode of mitochondrial DNA replication in cultured human cells, Nucleic Acids Res. 34 (20) (2006) 5815–5828.
[45] C.R. Chang, C. Blackstone, Dynamic regulation of mitochondrial fission through modification of the dynamin-related protein Drp1, Ann. N. Y. Acad. Sci. 1201 (1) (2010) 34–39.
[46] S. Nakamura, T. Takamura, N. Matsuzawa-Nagata, H. Takayama, H. Misu, H. Noda, S. Nabemoto, S. Kurita, T. Ota, H. Ando, Palmitate induces insulin resistance in H4IIEC3 hepatocytes through reactive oxygen species produced by mitochondria, J. Biol. Chem. 284 (22) (2009) 14809–14818.
[47] P.S. Brookes, Mitochondrial H+ leak and ROS generation: an odd couple, Free Radic. Biol. Med. 38 (1) (2005) 12–23.
[48] D.C. Wallace, Mitochondria and cancer, Nat. Rev. Cancer 12 (10) (2012) 685.
[49] A. Sandouka, E. Balogun, R. Foresti, B. Mann, T. Johnson, Y. Tayem, C. Green, B. Fuller, R. Motterlini, Carbon monoxide-releasing molecules (CO-RMs) modulate respiration in isolated mitochondria, Cell. Mol. Biol. 51 (4) (2005) 425–432.
[50] L. Braud, M. Pini, L. Muchova, S. Manin, H. Kitagishi, D. Sawaki, G. Czibik, J. Ternacle, G. Derumeaux, R. Foresti, R. Motterlini, Carbon monoxide-induced metabolic switch in adipocytes improves insulin resistance in obese mice, JCI Insight 3 (22) (2018).
[51] L.L. Iacono, J. Boczkowski, R. Zini, I. Salouage, A. Berdeaux, R. Motterlini, D. Morin, A carbon monoxide-releasing molecule (CORM-3) uncouples mitochondrial respiration and modulates the production of reactive oxygen species, Free Radic. Biol. Med. 50 (11) (2011) 1556–1564.
[52] T. Nishikawa, N. Bellance, A. Damm, H. Bing, Z. Zhu, K. Handa, M.I. Yovchev, V. Sehgal, T.J. Moss, M. Oertel, A switch in the source of ATP production and a loss in capacity to perform glycolysis are hallmarks of hepatocyte failure in advance liver disease, J. Hepatol. 60 (6) (2014) 1203–1211.